NAVAL POSTGRADUATE SCHOOL

MONTEREY, CALIFORNIA

THESIS

ARRAY BASED FREE SPACE OPTIC SYSTEM FOR TACTICAL COMMUNICATIONS

by

Adrian W. Felder

June 2018

Thesis Advisor: John H. Gibson
Co-Advisor: Gurminder Singh

Approved for public release. Distribution is unlimited.

THIS PAGE INTENTIONALLY LEFT BLANK

REPORT DOCUMENTATION PAGE			*Form Approved OMB No. 0704-0188*
Public reporting burden for this collection of information is estimated to average 1 hour per response, including the time for reviewing instruction, searching existing data sources, gathering and maintaining the data needed, and completing and reviewing the collection of information. Send comments regarding this burden estimate or any other aspect of this collection of information, including suggestions for reducing this burden, to Washington headquarters Services, Directorate for Information Operations and Reports, 1215 Jefferson Davis Highway, Suite 1204, Arlington, VA 22202-4302, and to the Office of Management and Budget, Paperwork Reduction Project (0704-0188) Washington, DC 20503.			
1. AGENCY USE ONLY ***(Leave blank)***	**2. REPORT DATE** June 2018	**3. REPORT TYPE AND DATES COVERED** Master's thesis	
4. TITLE AND SUBTITLE ARRAY BASED FREE SPACE OPTIC SYSTEM FOR TACTICAL COMMUNICATIONS			**5. FUNDING NUMBERS**
6. AUTHOR(S) Adrian W. Felder			
7. PERFORMING ORGANIZATION NAME(S) AND ADDRESS(ES) Naval Postgraduate School Monterey, CA 93943-5000			**8. PERFORMING ORGANIZATION REPORT NUMBER**
9. SPONSORING / MONITORING AGENCY NAME(S) AND ADDRESS(ES) N/A			**10. SPONSORING / MONITORING AGENCY REPORT NUMBER**
11. SUPPLEMENTARY NOTES The views expressed in this thesis are those of the author and do not reflect the official policy or position of the Department of Defense or the U.S. Government.			
12a. DISTRIBUTION / AVAILABILITY STATEMENT Approved for public release. Distribution is unlimited.			**12b. DISTRIBUTION CODE** A

13. ABSTRACT (maximum 200 words)

Free-space optical (FSO) communications offer a resilient and flexible alternative communications medium to current radio technologies, which are increasingly threated by our peer adversaries. FSO provides many advantages to radio technologies, including higher bandwidth capability and increased security through its low probability of detection (LPD) and low probability of interception (LPI) characteristics. However, current FSO systems are limited in range due to line-of-sight requirements and suffer loss from atmospheric attenuation.

This thesis proposes the use of arrayed optical emitters for FSO communication by developing a link-layer protocol that leverages the inherent error correction of quick response (QR) encoding to increase bandwidth and overcome atmospheric loss. Through the testing of a system built with commercial-off-the-shelf equipment and a survey of current optical transmitter and receiver technology, this link-layer protocol was validated and estimated to provide similar data rates to current single emitter FSO systems.

Various limitations were discovered in the current structure of the protocol. Future work should be conducted to correct inefficiencies in the QR encoding format when applied to a transmission medium. Additionally, technological advancements in hardware systems, including the large-scale production of VCSELs and faster high-speed cameras, must be achieved before such an FSO would be viable for large-scale use.

14. SUBJECT TERMS free-space optics, tactical communication, quick response code, laser communication, low probability of detection, low probability of interception, line-of-sight	**15. NUMBER OF PAGES** 105
	16. PRICE CODE

17. SECURITY CLASSIFICATION OF REPORT	**18. SECURITY CLASSIFICATION OF THIS PAGE**	**19. SECURITY CLASSIFICATION OF ABSTRACT**	**20. LIMITATION OF ABSTRACT**
Unclassified	Unclassified	Unclassified	UU

NSN 7540-01-280-5500 Standard Form 298 (Rev. 2-89)
Prescribed by ANSI Std. 239-18

THIS PAGE INTENTIONALLY LEFT BLANK

Approved for public release. Distribution is unlimited.

ARRAY BASED FREE SPACE OPTIC SYSTEM FOR TACTICAL COMMUNICATIONS

Adrian W. Felder
Captain, United States Marine Corps
BSME, Virginia Tech, 2011

Submitted in partial fulfillment of the
requirements for the degree of

MASTER OF SCIENCE IN COMPUTER SCIENCE

from the

NAVAL POSTGRADUATE SCHOOL
June 2018

Approved by: John H. Gibson
Advisor

Gurminder Singh
Co-Advisor

Peter J. Denning
Chair, Department of Computer Science

THIS PAGE INTENTIONALLY LEFT BLANK

ABSTRACT

Free-space optical (FSO) communications offer a resilient and flexible alternative communications medium to current radio technologies, which are increasingly threated by our peer adversaries. FSO provides many advantages to radio technologies, including higher bandwidth capability and increased security through its low probability of detection (LPD) and low probability of interception (LPI) characteristics. However, current FSO systems are limited in range due to line-of-sight requirements and suffer loss from atmospheric attenuation.

This thesis proposes the use of arrayed optical emitters for FSO communication by developing a link-layer protocol that leverages the inherent error correction of quick response (QR) encoding to increase bandwidth and overcome atmospheric loss. Through the testing of a system built with commercial-off-the-shelf equipment and a survey of current optical transmitter and receiver technology, this link-layer protocol was validated and estimated to provide similar data rates to current single emitter FSO systems.

Various limitations were discovered in the current structure of the protocol. Future work should be conducted to correct inefficiencies in the QR encoding format when applied to a transmission medium. Additionally, technological advancements in hardware systems, including the large-scale production of VCSELs and faster high-speed cameras, must be achieved before such an FSO would be viable for large-scale use.

THIS PAGE INTENTIONALLY LEFT BLANK

TABLE OF CONTENTS

THIS PAGE INTENTIONALLY LEFT BLANK

LIST OF FIGURES

LIST OF TABLES

THIS PAGE INTENTIONALLY LEFT BLANK

LIST OF ACRONYMS AND ABBREVIATIONS

3D	3-Dimensional
5G	Fifth Generation
AFRL	Air Force Research Laboratory
ARP	Address Resolution Protocol
BER	Bit Error Rate
COTS	Commercial-Of-The-Shelf
CPU	Central Processing Unit
DARPA	Defense Advanced Research Program Agency
DNS	Domain Naming Service
ECC	Error Correction Code
EEROM	Electronically Erasable Read Only Memory
EMI	Electromagnetic Interference
FEC	Forward Error Correction
FER	Frame Error Rate
FID	Fragment Identifier
FPS	Frames Per Second
FOENIX	Free Space Optical Experimental Network Experiment
FSO	Free Space Optics
HAT	Hardware Attached on Top device
HTTP	Hypertext Transfer Protocol
ICI	Inter Channel Interference
ICMP	Internet Control Message Protocol
IEEE	Institute of Electrical and Electronics Engineers
ILOS	Indirect Line-of-Sight
IP	Internet Protocol
IR	Infrared
LAN	Local Area Network
LED	Light Emitting Diode
LID	Link Identifier
LLI	Link-Layer Interface Module

LOS	Line of Sight
LPD	Low Probability of Detection
LPI	Low Probability of Interception
MAC	Medium Access Control
MIMO	Multiple-Input-Multiple-Output
NPS	Naval Postgraduate School
NRL	Naval Research Laboratory
NRZ	Non-Return-to-Zero
PCAP	Packet Capture file
PER	Packet Error Rate
PID	Packet Identifier
QOTR	QR Code Optical Transmitter Receiver
QR	Quick Response
RAM	Random Access Memory
RF	Radio Frequency
RPi	Raspberry Pi computer
RX	Receiver Module
RZ	Return-to-Zero
SCF	Sequence Control Field
SDRAM	Synchronous Dynamic Random Access Memory
SFD	Start Frame Delimiter
SISO	Single-Input-Single-Output
SPAWAR	Space and Naval Warfare Systems Command
SRAM	Synchronous Random Access Memory
TALON	Tactical Line-of-sight Optical Network
TB	Terminal Bit
TCP-IP	Transport Control Protocol-Internet Protocol model
TX	Transmitter Module
URL	Uniform Resource Locator
UV	Ultra-Violet
VLC	Visible Light Communication
WAN	Wide Area Network

ACKNOWLEDGMENTS

The journey to bring this research to fruition has been more than a year in the making and involved support from many different people. First and foremost, I would like to thank my advisors, John Gibson and Dr. Gurminder Singh. Their insight and mentorship was vital to the completion of my research. Additionally, Peter Ateshian and “The Interns” greatly helped in the development of the QOTR system, all the way from inception to testing. Your time and knowledge was greatly appreciated.

Next, I would like to thank my family members for their support throughout my time at NPS and during my Marine Corps career. Both my parents assisted in the editing of this thesis and acted as a valuable sounding board, as I melded it into the final state that it is in now.

I would also like to recognize the individuals at Naval Research Labs, SPAWAR, and the I MEF Science and Technology Office who supported my research. Thank you for your time, knowledge, and input, without which none of this work would have been possible.

Lastly, I would like to thank the Marines, Sailors, and civilians in my Computer Science cohort. The last two years has had its ups and downs. Through it all, I have not only learned far more than I ever expected about 1’s and 0’s, but also I’ve met an amazing group of professionals who I know I will call friends for the rest of my life. Without you all, there is a good chance that I would have lost my mind a long time ago.

THIS PAGE INTENTIONALLY LEFT BLANK

I. INTRODUCTION

Free-space optical (FSO) technology is a proven medium for network communications and has found its use in both commercial and military applications in the early 21st century. In terms of military applications, FSO communications present a solution to many problems now facing the U.S. armed forces, the largest of which being how the U.S. military enables robust and secure wideband network communications when combating a near-peer enemy able to wage war in the cyber domain. Traditional radio frequency (RF) communications fall short of this task, lacking the necessary bandwidth and security to protect against cyber attacks while simultaneously providing enough throughput to support the data-intensive requirements of the modern battlespace. For this reason, there has been a large push by the Department of the Navy in recent years for FSO research and experimentation, such as the development of systems like the Marine Corps' Tactical Line-of-sight Optical Communications Network (TALON) system.

Utilizing the optical frequency spectrum, FSO communications for military applications offer the advantages of having a low probability of detection (LPD), low probability of interception (LPI), and data rates up to orders of magnitude faster than RF links. While terrestrial FSO systems lack the range that can be attained using troposcatter or satellite RF communications, this limitation can be overcome by the use of aerial- or ground-based repeater sites. Research continues to be conducted into extending FSO range by mitigating the atmospheric effects that limit FSO signal strength.

The majority of FSO systems currently being tested and fielded for military applications are single-input-single-output (SISO) devices; however, another possible configuration for FSO systems is multiple-input-multiple-Output (MIMO). Compared to SISO systems, MIMO systems theoretically can support greater bandwidth capability and higher link availability, at the cost of higher power consumption. When coupled with error correction techniques, and technologies

such as machine learning, MIMO may be able to increase link efficiency and range for tactical communications.

A. PROBLEM STATEMENT

The purpose of this thesis is to determine whether a MIMO FSO transmission system provides value to tactical network communications and what capabilities and limitations may be for such a system built with commercial-off-the-shelf (COTS) materials.

B. OBJECTIVES

The key objectives of this thesis are (1) to understand MIMO FSO and its advantages and limitations; (2) to design, construct, test, and evaluate a MIMO FSO system using commercial-off-the-shelf equipment (COTS); and (3) to design and execute experiments that evaluate the performance of this MIMO FSO system and analyze the results.

C. SCOPE

This thesis focuses on the design, construction, and testing of a MIMO FSO system. The resources and capabilities of Naval Postgraduate School (NPS) personnel, equipment, and funding limit the size and range of this device. Where specific testing is not feasible, this thesis attempts to research the likely implications such testing would have and proposes future work on the subject.

D. ORGANIZATION OF THESIS

The remainder of this thesis is organized into four chapters. Chapter 2 covers the background of various technologies and concepts applicable to the development of a MIMO FSO system. Chapter 3 outlines the system design of a MIMO FSO system constructed with COTS equipment. Chapter 4 discusses the conduct of these experiments and the analysis of the results. Lastly, Chapter 5 offers the conclusions of the thesis and recommended directions for future work in this field of study.

II. BACKGROUND

This chapter provides background related to MIMO FSO communication. For the purposes of this thesis, MIMO refers to a communications link that uses multiple laser transmitters operating in parallel to transmit one stream of data and multiple receivers to receive this data and re-aggregate it at the distant end of the link. This chapter starts with a review of the theory and main concepts of FSO, touching on technologies within the field that are relevant to tactical applications. It then addresses the types of equipment available for FSO transmission and reception. Finally, it presents concepts of employment for a MIMO FSO system.

A. FSO FUNDAMENTALS

Operating in the optical frequency spectrum, FSO provides many advantages over RF, making it well suited for military applications. The vast majority of FSO transceivers in use or under development by the military operate in a SISO configuration. However, the fundamental concepts of FSO apply similarly to both MIMO and SISO links.

1. The Optical Frequency Spectrum

FSO systems operate using the optical frequency spectrum, defined as wavelengths between 100 nm to 3100 nm. Consisting of a series of frequency bands that operate above the RF spectrum but below x-ray and gamma ray wavelengths, the optical frequency spectrum includes infrared (IR), visual, and ultraviolet (UV) light. Wireless optical telecommunications uses four bands, as shown in Figure 1. Note that wavelengths are longer as frequency is lower.

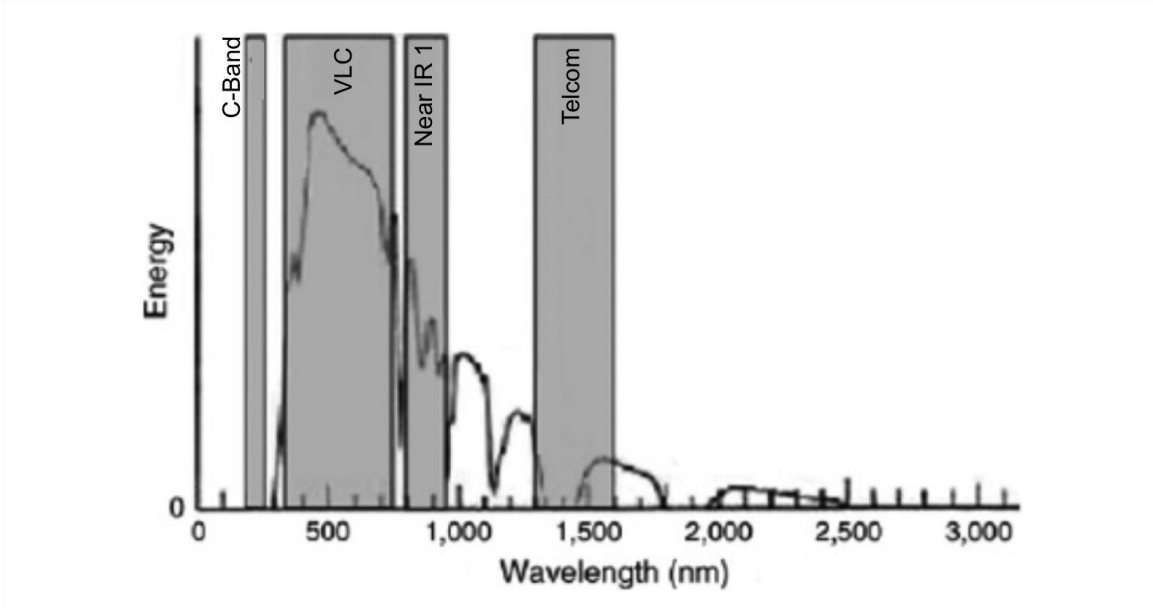

Figure 1. Illustration of the Optical Spectral Bands. Adapted from [1].

The bands most applicable to this thesis are telecom and visual light communication (VLC) bands. Most tactical FSO systems operate at wavelengths inside the telecom band, also known as long-wavelength beams [2]. Because these wavelengths are below the visible light frequency, they provide the best LPI and LPD characteristics. More information on current tactical FSO systems is available in “Appendix A. Survey of Tactical FSO Systems.”

The VLC band uses short-wavelength beams and contains light visible to the human eye. Short-wavelength beams are typically used for underwater FSO (blue and green wavelengths). Red lasers are commonly used for testing and experimentation because of the visual reference they produce and their availability. This thesis will use the VLC band for these reasons; however, all technologies used are theoretically transferable to non-visible, longer-wavelength optical beams as a consideration for future tactical use.

2. System Topology

The system topology of an FSO link is very similar to an RF link and includes five major components: a source modem, a source transceiver, the

optical channel, a destination transceiver, and the destination modem [3]. Figure 2 shows the equipment string of a typical FSO link. This thesis focuses on developing a transmission system that provides for all elements of this topology, using light emitting diodes (LEDs) as the optical channel.

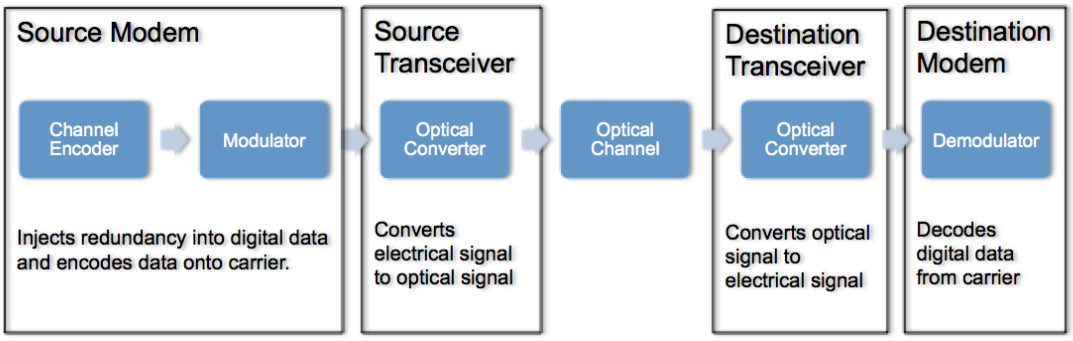

Figure 2. FSO Link System Topology for a Digital System. Adapted from [3] and [4].

a. Channel Encoding

Channel encoding is the process of inserting redundancy into a digital signal in order to overcome transmission errors. Channel encoding is especially important for FSO links due to the large effect that atmospheric conditions can have on data transmission. These conditions are discussed in more depth later in this chapter. FSO modems commonly use coding techniques that include forward error correction (FEC), convolutional codes, and/or concatenated codes as error correction techniques [3]. With proper implementation, manipulation of transmitted packets with these codes can enable the destination modem to reconstruct corrupted packets. However, implementation of any error correction code (ECC) does reduce the effective throughput of a link because of the additional bandwidth required for the added data redundancy.

Another method of correcting for transmission errors that is commonly used in FSO is temporal diversity. Temporal diversity is the process of sending the same packet multiple times across a link to ensure delivery and can be

extremely effective at reducing error rates. However, proper implementation of temporal diversity has high bandwidth costs, often requiring nearly half of the available bandwidth for error correction [5].

This thesis seeks to use the Quick Response (QR) code format to accomplish channel encoding. The QR code format gives the user the option of encoding data with 7%, 15%, 25%, or 30% redundancy for error correction and offers great flexibility and bandwidth management [6] [7]. More information on this technology can be found in “Appendix B. QR Encoding.”

b. Modulation

Modulation is the process of mapping information onto a carrier. In the case of FSO, this is typically done digitally, with the most common method being on-off keying (OOK). OOK uses variations in the laser transceiver’s power output to represent binary digits and can be applied in either return-to-zero (RZ) or non-return-to-zero (NRZ) formats. The advantage of OOK for FSO is its simplicity and nonlinearity. Each pulse of a binary digit has the same symbol duration, allowing for relatively easy synchronization between transmitter and receiver [3]. To map NRZ or RZ signal onto a carrier, the carrier waveform and binary signal are combined to produce the electrical signal to be transmitted, shown in Figure 3. In the case of FSO, the carrier waveform is the optical wavelength and the OOK modulated signal becomes that carrier waveform turning on and off.

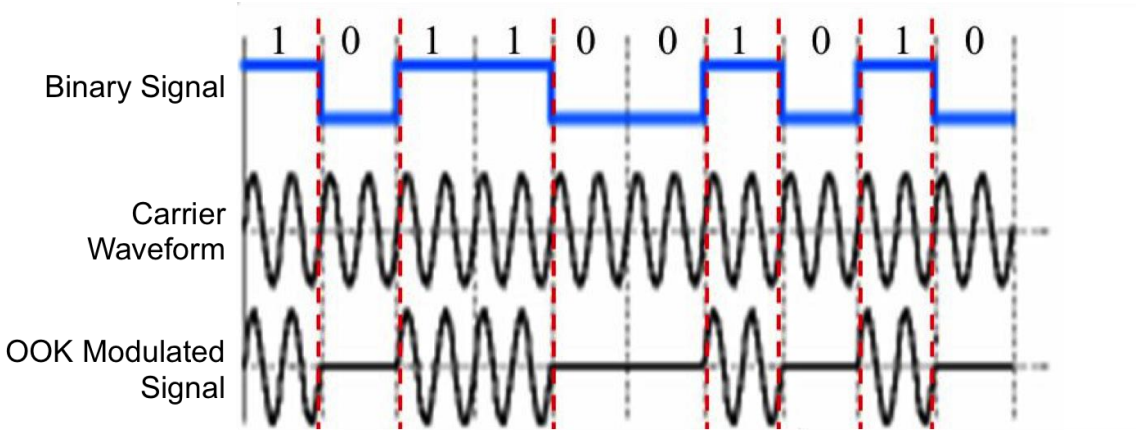

Figure 3. NRZ OOK Modulation Process. Adapted from [3].

Another type of optical modulation that has been in use since before the advent of computers is Morse code. Morse code uses sequences of long and short optical pulses (dots and dashes) to transmit text information from an optical transmitter to and optical receiver. Because of the simple nature of Morse code, applying it in an FSO system avoids the need for a complex modem to map the data onto the carrier. Instead, this mapping can be accomplished by simple code, making it an ideal modulation style for experimenting with simple FSO configurations. While the overall data rates of a Morse code style FSO system will be lower than that of systems that use modems, the technique is valuable for observing the data rates of SISO and MIMO systems in order to compare their performance.

3. Advantages of FSO

FSO provides many advantages for tactical applications, including potentially higher bandwidth than RF systems, LPI and LPD qualities, and frequency availability. Most of these advantages are a result of the characteristics of the optical frequency spectrum and include higher bandwidth, LPI and LPD, and the use of an unmanaged frequency spectrum.

a. Higher Bandwidth

Because of the shorter wavelength of optical waveforms as compared to RF frequencies, a FSO link has the capability to carry far more data. Laboratory and commercial FSO systems have demonstrated bandwidths in the high gigabit range, with some systems reaching terabits per second (Tbps) [3]. In recent years, tactical FSO systems have demonstrated link data rates in excess of 1 gigabit per second (Gbps) [8]. More information on relevant tactical FSO systems can be found in "Appendix A. Survey of Tactical FSO Systems." In all of the cases studied, the systems are SISO. From the demonstrated bandwidths, similar MIMO systems are theoretically expected to achieve data rates in the terabit per second range when implementing one hundred or more laser diodes in parallel.

b. LPI and LPD

For tactical applications, FSO communications are extremely appealing because of the low signature they produce. While RF communications systems typically propagate their signals in wider beams that are easily intercepted, FSO systems use very narrow beams. Their transmitted energy can be focused to very small spot sizes, greatly reducing the probability of an enemy detecting or intercepting the transmission. If an adversary were to detect and then attempt to eavesdrop on the signal, this would cause signal interference that would likely reduce the power received at the receiving side of the link enough to shut down data transmission and indicate an attempt to interfere with the link [9].

In addition to its LPI and LPD characteristics, an FSO link is immune to either accidental or purposeful interference caused by radio frequency interference due to its operating outside of the radio frequency spectrum [10].

c. Unmanaged Frequency Spectrum

While the radio frequency spectrum is highly regulated by regional, national, and international entities, the optical frequency spectrum is currently

unmanaged due to the ability for similar optical links to operate in close proximity with one another without causing interference. Because of this freedom and the increasing congestion of the RF spectrum as fifth generation (5G) technologies mature, optical links are seen as a valuable option for the more dynamic military communications networks [11].

4. Disadvantages of FSO

Despite the many useful advantages, FSO does have some drawbacks. The majority of the disadvantages of FSO communications are derived from the environment within which these systems are employed. These include the line-of-sight (LOS) nature of optical signals and limited availability.

a. Line-of-Sight Limitations

The major disadvantage of FSO technology is that it is reliant on a clear LOS, even more so than some RF bands because of the much shorter wavelength of the optical bands. Any physical obstruction can degrade or cut off an FSO link, including particles in the atmosphere, which are discussed in the "Environmental Effects" section in this chapter. Common methods of overcoming line of sight issues are by gaining elevation for the transceiver and utilizing repeater sites. In terrestrial FSO links, at a minimum, the curvature of the Earth sets the boundary for the effective ranges of transmitters, with the longest ground and sea-based systems being approximately 70 km [3].

b. Limited Availability

Availability is the ratio of the time a network is actually delivering services to the time it is expected to be delivering services, often expressed as a percentage. FSO systems typically have much lower availability than RF links because of FSO's reduced resilience to atmospheric effects, which are discussed in the next section. In assessing the transmission impacts of these effects, Naval Research Laboratory (NRL) estimated one of its systems to have a short-term (approximately twenty-four hours) availability of 90% and a six-month availability

of 76%. A comparable RF link would have an availability in the high 90% range [9].

While there is little documented testing for availability of MIMO FSO systems specifically, it is expected that this type of system would improve upon these numbers because of the spatial diversity involved.

5. Environmental Effects

The majority of disadvantages associated with FSO systems are related to the negative effects that the environment has on these links. The effects that have the largest impact on an FSO beam are scintillation, absorption, and scattering.

a. Scintillation

Scintillation is a phenomenon caused by minute temperature variations in the air pockets through which a beam travels, which in turn causes fluctuations in the beam itself [12]. This results in an irregular distribution of energy at the receiver. Scintillation is most common in ground-to-ground links when there is a large amount of reflected heat from the sun [4]. The effect of scintillation is best understood when one considers that a mirage is the visual result of a scintillated link or the twinkling of starlight, the result of the scintillation through the atmosphere; this effect is due to changes in the atmospheric density through which the light has travelled [3].

b. Scattering

Scattering occurs when beam radiation is dispersed in a range of directions after physically interacting with an object. In terrestrial FSO, scattering is caused by particles in the atmosphere, including fog, smoke, dust, precipitation, aerosols and gases. Depending on the prevalence and size of these particles, scattering can greatly reduce the received power of an FSO beam [12]. In certain cases, for example where fog may completely obscure a link, beam power can be increased to overcome the scattering [13].

c. Absorption

Similar to scattering, absorption occurs when beam radiation collides with an atmospheric particle. If the resonate frequency of this radiation is the same as the beam, absorption causes the some of the beam's energy to be absorbed by the radiation. It also has an effect on the received power of the beam [12].

B. MULTIPLE-INPUT-MULTIPLE-OUTPUT CHANNELS

The concept behind MIMO for FSO communications is to overcome many of these environmental effects by using spatial diversity [14]. During modulation, the data to be transmitted is inverse-multiplexed so it can be spread across multiple transmitters. At the receiving end, the data is then de-multiplexed to reconstitute the data. A comparison of SISO and MIMO FSO is illustrated in Figure 4. MIMO FSO transmitters vary in the number of lasers they employ. In a laboratory setting, a MIMO system using 16 lasers has been proven effective over a distance of 5 meters with a bandwidth of 100 Gbps [14]. With an increased size for the laser array both in the number of lasers used and the distance between lasers, further bandwidth and diversity can be achieved.

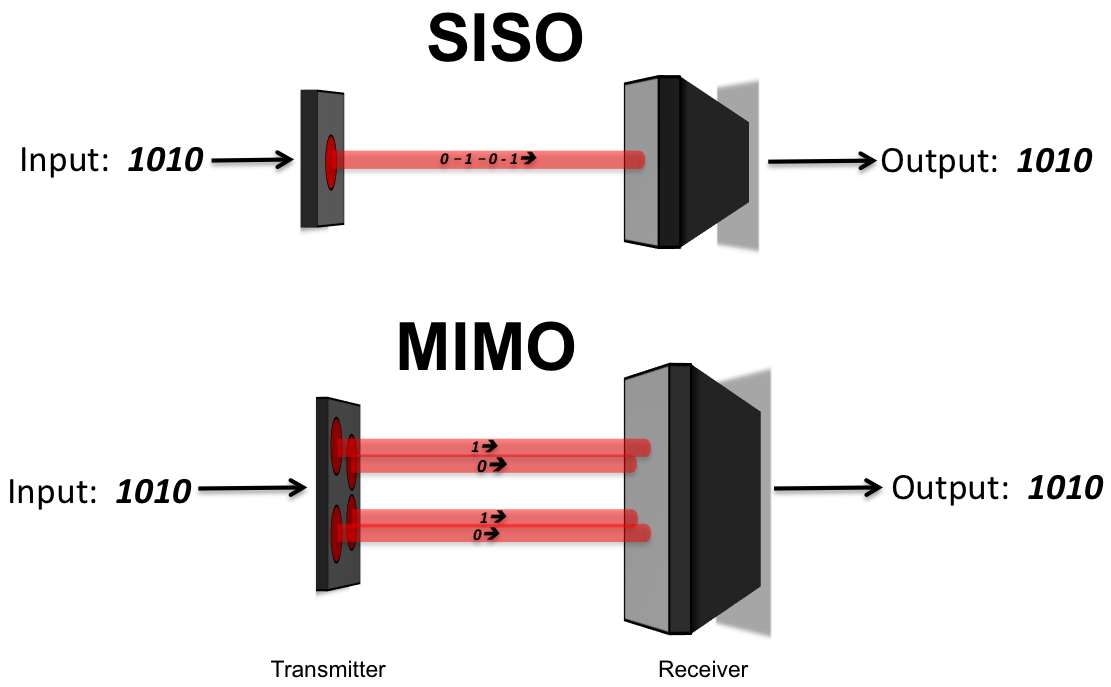

Figure 4. Illustration of SISO and 4-Laser MIMO FSO Implementation. Adapted from [15] and [14].

1. Advantages of MIMO over SISO

The primary advantage of a MIMO configuration is that the spatial diversity of lasers can mitigate some of the environmental effects to which FSO links are subject, resulting in greater link availability. The more spatial diversity applied to the system, the more atmospheric loss can be reduced. Additionally, MIMO links can theoretically have larger bandwidths because they use multiple lasers, either by combining the parallel beams to increase the signal-to-noise ratio or transmitting different data streams on each laser [15]. The nature of MIMO systems, when coupled with other relevant technologies such as QR code and optical camera receivers, allows for many flexible methods of employment beyond typical point-to-point FSO systems. Descriptions of these topologies can be found in “Appendix C. Concepts of Employment.”

2. Disadvantages of MIMO over SISO

The increased bandwidth and availability of MIMO links come at an increased cost of power, capital expense, and inter-channel interference (ICI). A MIMO system containing N lasers will consume N times as much power as a SISO system operating with the same type of laser. The same direct relationship exists with equipment cost. It should be noted that this relationship might not hold true for the amount of power that reaches the distant receiver due to atmospheric attenuation and ICI. ICI is a phenomenon that occurs when lasers operate at the same wavelength and travel along the same vector while in close proximity, which is what a MIMO laser array produces. This interference can result in data loss along the link [14]. ICI will be more prevalent at longer ranges where beam divergence has a greater effect. Beam divergence is defined as the angle at which the beam diffracts from the aperture centerline [3]. To overcome ICI, beams in the MIMO array should have less beam divergence, thus requiring a more complex laser source.

3. MIMO Bandwidth Potential

As discussed previously, a MIMO FSO system offers great bandwidth potential because it places many beams in parallel with each other. Each of these beams is capable of transmitting at least 1 to 10 Gbps of data using OOK modulation, as demonstrated in a previous NPS thesis [4]. This thesis looks at using QR codes as a form of channel encoding for a MIMO system. The minimum size of a QR code is a 21 by 21 array, or 441 individual data points, as shown in Figure 5. For more information on QR Codes, see “Appendix B. QR Encoding.”

Figure 5. Example 21 by 21 QR Code. Source: [7].

To use QR encoding in an FSO system will require an array of 441 laser diodes. If we consider that each one of these diodes is only capable of the floor of the proven bandwidth, 1 Gbps, it can be concluded that this type of FSO system has a theoretical bandwidth of 0.44 Tbps. It should be noted that this is the overall capacity of the link. The useable throughput of such a link would be less because of the signaling and error correction that is resident in each QR code that is transmitted.

C. OPTICAL SYSTEM COMPONENTS

The primary components that set FSO systems apart from RF systems are the means of transmission and reception. In this section, the various technologies used to accomplish these tasks are presented.

1. Optical Transmission

This thesis seeks to use LEDs for optical transmission to develop a system and protocol that can support laser diode transmission in future research. The characterization of a laser, beyond the wavelength at which it operates, is determined by its power output and beam divergence [16]. A laser operating at a higher power and smaller beam divergence will have a longer range and higher bandwidth capability, at the cost of higher power consumption and higher manufacturing cost.

Laser diodes come in various types, but the type researched for this thesis is vertical-cavity surface emitting lasers (VCSELs). VCSELs provide high-speed operation at high power and high reliability and efficiency [17]. They produce circular beams, as opposed to elliptical beams resulting in improved coupling efficiency with the optical receiver. While early VCSEL technology was primarily in the VLC band, further development has produced VCSELs operating in the Telecom band and has demonstrated bandwidths beyond 3 Gbps [17].

2. Optical Reception

FSO systems typically use one of two methods to receive data: optical imagery or photodiodes. The purpose of both is to collect the transmitted photons and reconstruct the data that they represent. However, the two methods accomplish this task in different ways. This thesis focuses on optical imagery devices for reception because of the need when using MIMO to receive and process multiple beams at the same time.

Any camera can operate as an optical receiver. When the laser is pointed at the camera, images are captured, and the wavelength of the beam is isolated using imaging software to read the transmitted data. The limitation of optical imagery on the data rate of an FSO link is the frame rate at which the camera operates. If the laser is transmitting at a faster rate than the camera can view, data will be lost. In addition, a camera with optical or digital zoom, similar to a telescope, can increase the effective range of the FSO system.

For establishing a MIMO FSO link, an optical receiver with an extremely high frame rate will be required to achieve link data rates in the Gbps and Mbps ranges. A survey of the current cutting-edge ultra high-speed cameras is shown in Table 1. It was found that commercial systems are currently capable of recording at rates around 100 thousand frames per second (FPS) for QR image resolutions

Table 1 Survey of Commercial Ultra High-Speed Cameras. Adapted from [18], [19], and [20].

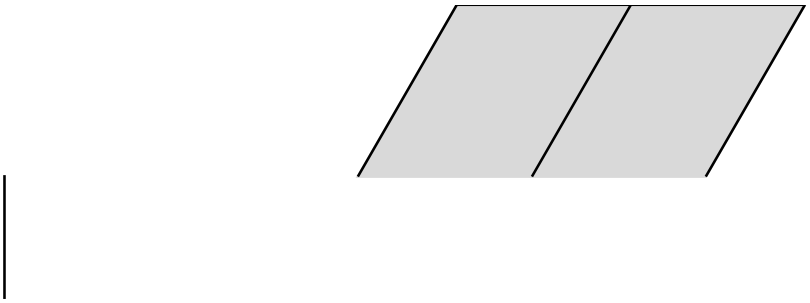

Advantages to using a camera for reception include the possibility to use both an optical zoom and a wider aperture for pointing. Selecting a camera with an optical zoom can increase the detection range of FSO. Imaging software can further improve reception and is necessary if the FSO seeks to employ a MIMO system with only one camera receiver in order to process multiple beams from the same image.

D. NETWORKING CONSIDERATIONS

To integrate the physical link with a tactical wide area network circuit, a MIMO system must have a network interface with the TCP-IP model. In this sub-section, the pertinent elements of the TCP-IP model in regards to such a system are discussed. As with all network transmissions systems, FSO systems operate at the physical and link layers of the model. The system does not interact with the network layer because it is payload agnostic.

1. Link-Layer

The system in this thesis operates at the link-layer when receiving and transmitting data frames. The link-layer provides the services of framing, link access, and reliable delivery to datagram transmission. Link access, implemented with medium access control (MAC), is relatively simple for FSO links because of their point-to-point nature. Because the proposed system architecture consists of two separate simplex links, there is no need to de-conflict

between sending and receiving, as the two simplex links form a full-duplex capability.

For the purposes of FSO transmission, two of these are important to understand in depth: framing and reliable delivery. The process of encapsulating a network-layer datagram into a link-layer frame is framing. Nearly all link-layer protocols use some type of framing prior to transmission over a link in order to standardize the way data is sent. Two of the most common link-layer protocols that do framing are Ethernet and Wi-Fi. The structure of such frames is determined by the IEEE protocol standard [21].

The second service we employ at the link layer in FSO is reliable delivery. Reliable delivery in the link-layer is defined as the ability to move a network-layer datagram across a link without error. Link-layer protocols differ in the way they achieve this as well as how well they are able to deal with error correction. For protocols that are more prone to high error rates, such as Wi-Fi, more emphasis is placed within the protocol on error correction in order to make transmission more resilient. Less error prone links, such as over coaxial cable or fiber, do not provide any reliable delivery service because of the inherent reliability of the physical medium [21]. As reference for developing a format for MIMO transmission, the 802.2 Ethernet and 802.11 Wi-Fi frames were analyzed to determine possible solutions. These formats were chosen because of their widespread use and similar implementations.

a. 802.3 Ethernet

The IEEE 802.3 Ethernet protocol is a valuable protocol to leverage because it is commonly used for point-to-point links, such as with switched Ethernet. An Ethernet frame is able to transport packets of up to 1500 bytes using a combined overhead of 26 bytes, including the 8-byte preamble/start-of-frame-detection fields used to synchronize the sending and receiving devices. The Ethernet frame structure is shown in Figure 6 and described in detail below.

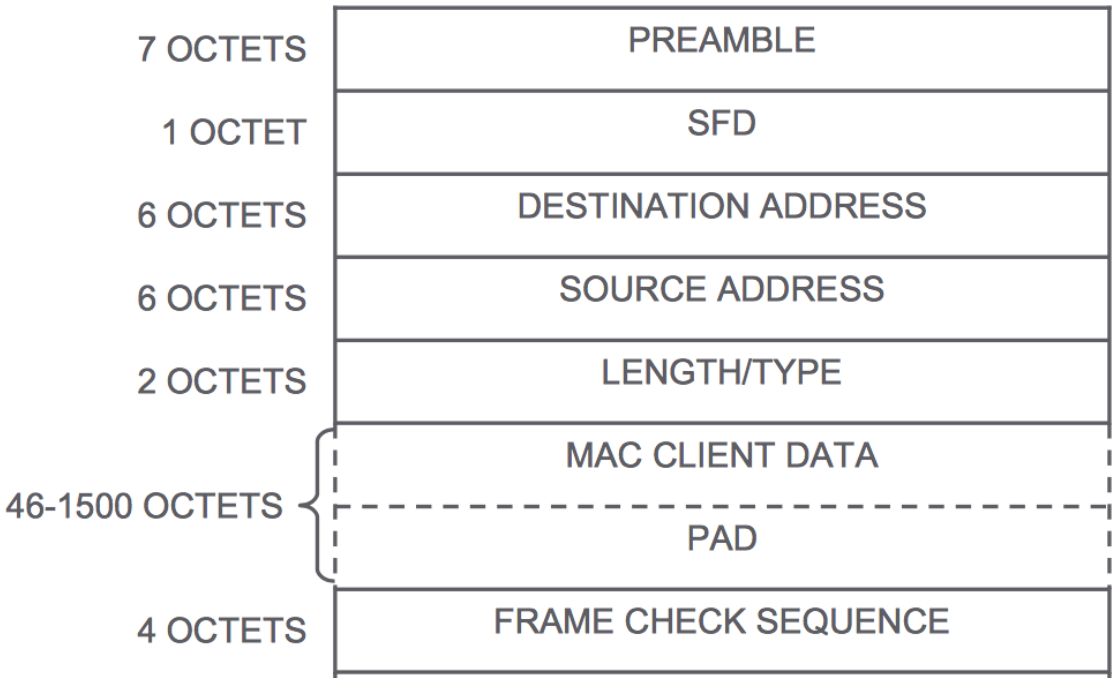

Figure 6. 802.3 Ethernet Frame Structure. Source: [22].

(1) Preamble

The preamble is a seven-byte element used for signaling at the physical layer, ensuring correct timing and synchronization at the receiver [22].

(2) Start Frame Delimiter

The start frame delimiter (SFD) is a one byte, constant marker in every Ethernet frame that is used to separate the preamble from the rest of the MAC Frame. The SFD is always set to 10101011 [22].

(3) Destination and Source Addresses

Six bytes each are allocated for the source and destination addresses. These are the addresses assigned to the Ethernet interfaces of the respective devices [22].

(4) Length/Type

When this two-byte field is set to 1500 or less it indicates length of the payload in bytes. When it is set above 1500, it indicates the EtherType of MAC client protocol [22]. These designations are mutually exclusive.

(5) Frame Check Sequence

The frame check sequence, a four-byte field, is placed at the end of the frame to provide a cyclic redundancy check. The value is derived as a function of the contents of the MAC frame [22].

b. 802.11 Wi-Fi

The IEEE 802.11 protocol is valuable to the application of QR optical transmission because it operates in a wireless configuration, similar to FSO systems. While the IEEE 802.11 operates in multicast architecture, as opposed to the point-to-point nature of architecture of FSO links, there are concepts of this protocol's frame structure that we adapt to this thesis. The IEEE 802.11 Wi-Fi frame format is shown in Figure 7. The payload capacity of each frame varies depending on the version of the protocol, as does the protocol overhead size. The fields of the overhead valuable to FSO transmission are the four address fields and sequence control field [23].

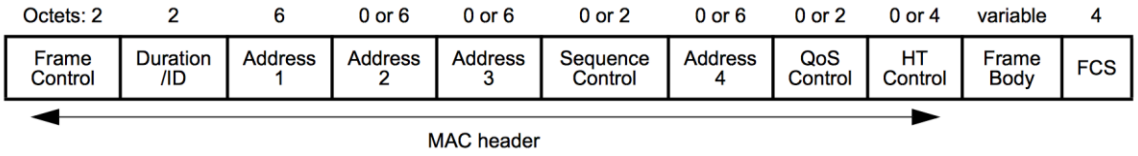

Figure 7. 802.11 Wi-Fi Frame Structure. Source: [23].

While two of the address fields in IEEE 802.11 are allocated for the source and destination MAC addresses, similar to Ethernet, the other two fields are used for the network basic service set identifier (BSSID) and the transmitter and receiver station addresses (optional) [23]. The inclusion of the BSSID is critical

because it ensures that only devices on the designated Wi-Fi network receive the frame, even when there are various Wi-Fi networks operating in the same frequency range.

The sequence control field (SCF), two bytes long, is used when the packet being sent is too large to be included in a single frame. The SCF contains two values, the sequence number (12 bit) and the fragment number (4 bit). Each packet is given a unique sequence number, which is inserted into the resulting frames (fragments). Each frame transmitted containing a portion of that packet has a fragment number, starting with 0 and incrementing by 1 each time. This ensures that frame payloads are reassembled correctly into whole packets at the receiver [23].

2. Protocol Design Considerations

That application of QR encoding for transmission will occur primarily at the link-layer. The system must encode and transmit payloads via QR code, where the payloads are IP packets. To do this, the link layer must attach signaling information to the packets and then fragment them to fit in a QR code's capacity. Drawing from the structure of Ethernet and Wi-Fi frames, as well of the concept of fragmenting from IPv4, the structure of the QR specific segmenting will be designed with the following considerations.

a. Segment Size

QR codes are the centerpiece of this system. Therefore, the size of each fragment will be limited to the capacity of a QR code. This capacity can vary depending on the QR code version and the error correction type, the smallest capacity of a 29 by 29 QR being 17 bytes (30% error correction) [7]. Maximizing the amount of this capacity that is used for payload instead of frame control operations is essential to increasing the useful bandwidth of the system.

b. Addressing

The link layer traditionally uses MAC addressing for its physical interface. However, because QOTR links are point to point and the size of the header must be minimized, non-MAC style addressing should be considered in order to negate the need for two six-byte address blocks in the head. This addressing should still retain the functionality of ensuring that the correct QOTR terminals are forming the link.

c. Sequencing

The limited capacity of each QR code requires that most IP packets be broken down into multiple payloads. Information in the frame header is needed to reconstruct these packets at the receiver side. The SCF in 802.11 offers a good example of how to do this while simultaneously providing a level of reliable delivery that the link-layer supplies.

E. SUMMARY

The FSO systems designed and tested in this thesis rely heavily on these basic concepts for optical energy transmission and reception. The ultimate employment of a QR-based encoded MIMO FSO system will combine the already proven technologies of laser diodes, QR codes, optical semiconductor reception, and mechanisms to mitigate the impairments of atmospheric transmission mediums.

THIS PAGE INTENTIONALLY LEFT BLANK

III. SYSTEM DESIGN

This chapter outlines the design of a QR-based MIMO FSO system. It discusses physical and logical construction of this system and decision points involved in the design process. While the system is built around LED optical transmission, the overall purpose of this testing is to determine the viability of a future arrayed laser/QR Code FSO system by testing the bandwidth, link availability, and performance of various technologies necessary for its future implementation.

The QR Code Optical Transmitter Receiver LED system (QOTR/LED) was designed using COTS equipment. Because of resource limitations, a QR-sized array of VCSELs was not available; instead, 32x32 LED arrays were used to project QR codes to optical receivers in a system known as QOTR/LED. This experiment's purpose is to serve as a technology demonstrator in order to send network information across this LED array/optical link. The QOTR/LED system architecture is shown in Figure 8, depicting the system architecture of two separate transmission systems, thus full duplex, and their integration with a tactical network.

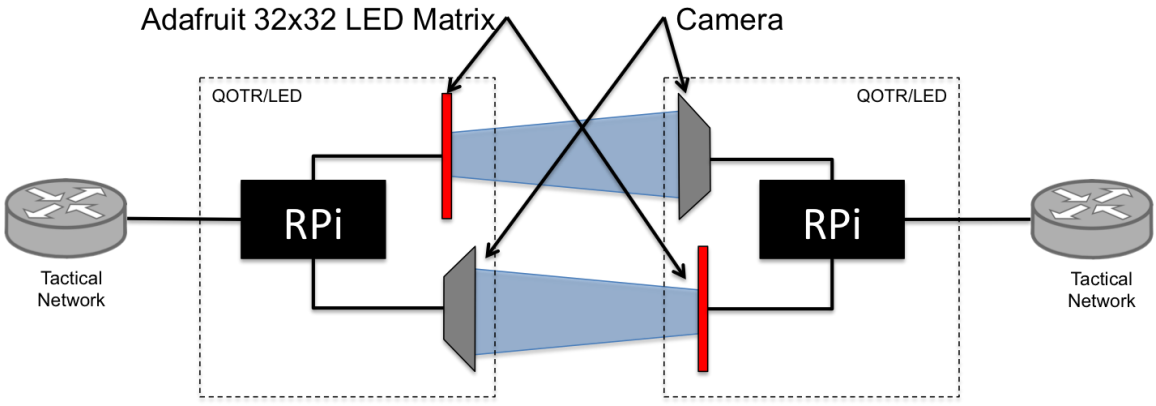

Figure 8. QOTR/LED Link Architecture.

A. HARDWARE

The QOTR/LED was designed with commercial-off-the-shelf equipment for economy and ease of development. All components are available on the open market and can be purchased for a relatively low cost.

1. Raspberry Pi 3

Currently, the most advanced version of Adafruit's Raspberry Pi (RPi) computer line, the RPi 3, as shown in Figure 9, was chosen because of its relatively high processing power, its ease of use, and its compatibility with other devices in the system architecture. The RPi's used for the QOTR/LED run four AMDv7 processors, totaling 1.2 GHz of processing power. Each central processing unit (CPU) has 16 GB of flash memory and 1 GB of synchronous dynamic random access memory (SDRAM) [24].

Figure 9. Raspberry Pi 3. Source: [25].

While adequate to conduct the experimentation for the QOTR/LED, a CPU with greater power and memory is preferred for future use. The RPi 3 was ideal

for the basic architecture because of its simple interface with the Adafruit 32x32 LED Matrices used to form the optical transmitter.

2. Adafruit 32x32 LED Matrix

The Adafruit 32x32 LED Matrix was chosen as the transmitter for the QOTR/LED because of its ease of use and its size relative to QR formats. Consisting of 1024 LEDs, the matrix is able to display up to 29x29 QR codes. Using the same drivers, four matrices can be used together to display up to 59x59 QR codes. Running on a 2A power supply, the matrix displays in full color with 4092 colors. Figure 10 shows a 32x32 matrix with RPi HAT (hardware attached on top) [25].

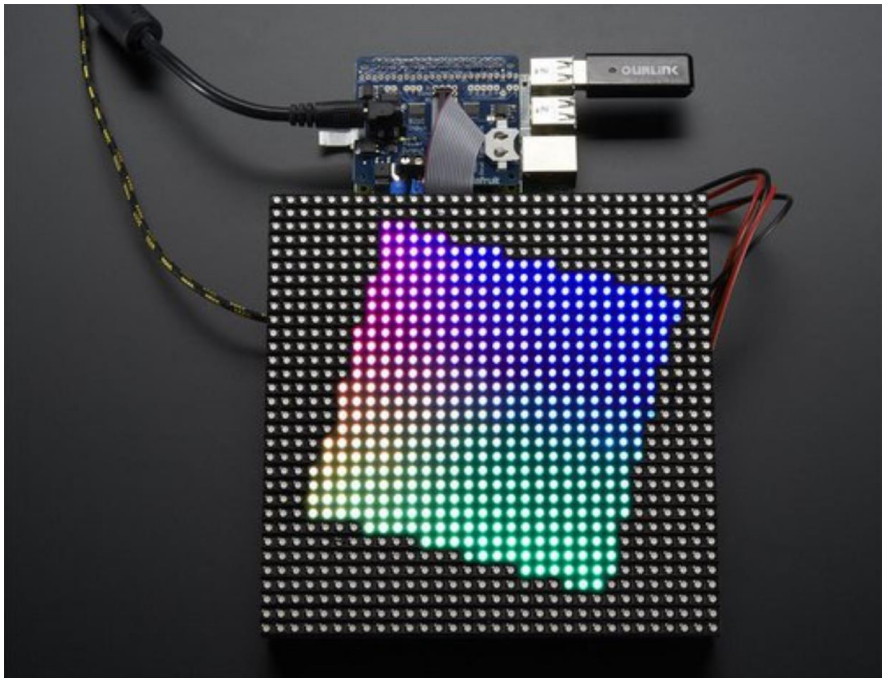

Figure 10. Adafruit 32x32 LED Matrix with Attached RPi HAT. Source: [26].

The LED matrix attaches to the RPi using an Adafruit RGB Matrix + Real Time Clock HAT, which enables a simple interface between the two devices using a 16-pin data cable [26].

3. Logitech HD Pro Webcam C920

The Logitech HD Pro webcam was selected as the optical receiver for the QOTR/LED system because of its high quality, ready availability, and reasonable cost. It is a medium- to high-cost webcam that is capable of recording video at 30 frames per second (fps) for 1080p and 60 fps for 720p. Connection to a CPU is done using a universal serial bus (USB) cable and it easily interfaces with the RPi operating system.

B. SOFTWARE

Python 2.7 was selected as the primary software language for coding the QOTR/LED. Python was selected because of its ease of use on RPi and the plethora of libraries available. The limiting factor that forced the use of Python 2.7 over Python 3 was the Adafruit RGB Matrix library, used to drive the LED matrix and Adafruit HAT, which is only available in Python 2.7.

1. Python Libraries

Various Python libraries are integral to the QOTR/LED software. All are open source and available from the cited sources.

a. PyQRCode

PyQRCode is a Python library that efficiently creates QR codes. It is used in the QOTR/LED transmitter. The Python library supports creation of version 1 through version 40 QR codes at L (7%), M (15%), Q (25%), or H (30%) levels of error correction. It is able to support QR encoding in all four modes of data; numeric, binary, alphanumeric, and kanji (Japanese). However, the supported characters in alphanumeric and kanji are extremely limited. Both text and image rendering of created QR codes are available [27].

See “

Appendix B. QR Encoding” for more information on QR formatting.

b. Adafruit RGB Matrix Library

The Adafruit RGB Matrix Library is a Python-wrapped, C++ library designed to work with the Adafruit RGB Matrix + Real Time Clock HAT. It provides a variety of prebuild functions and classes used to drive the Adafruit 32x32 LED Matrix. [26]

c. Zbar-Py

Zbar-Py is open source barcode reading software. Capable of reading both 1-dimensional and 2-dimensional barcodes and consisting of C++ code in a Python wrapper, it was an ideal library to be used in the QOTR/LED receiver. Zbar-Py is able to read a provided NumPy array and identify the presence of most QR codes. Version 1.0.4 was used, which is capable of processing QR codes of version 1 through 40 in the four most common error correction levels [28].

d. OpenCV-Python

The OpenCV-Python library provides capabilities to manipulate and display images. The QOTR system uses this library at the receiver side as a means to capture image frames from the receiver webcam and transfer them to Zbar-Py for processing. In this implementation, the conversion from the OpenCV Image format to the Numpy array required by Zbar-Py was done using the Python Image Library (PIL). Version 3.4.0.12 of OpenCV-Python was used [29].

e. Scapy

Scapy is a Python library used for traffic analysis. It provides functionality to analyze all layers of frame, including link-layer through applications-layer protocols. For the purpose of this thesis, the library is valuable in enabling the QOTR system to read and process real-time packets from the RPi Ethernet port and transmit them across the optical link, as well as writing the received packets to the Ethernet port on the receiving end. Version 2.3.2 was used [30].

2. Architecture

The software implementation for the QOTR/LED includes three main modules: the link-layer interface, the transmitter, and the receiver. Figure 11 shows the high level data flow of both network data and control data through the system. The Link-Layer Interface Module (LLI) is at the top of the architecture hierarchy; it is through this module that all operator interactions are conducted. The LLI controls the operation of both the Transmitter Module (TX) and the Receiver Module (RX). The entire system leverages Python's built in multithreading and multiprocessing modules to load balance processes. In order to initiate a QOTR/LED link, the operator provides the LLI with the desired QR version and ECC as well as a link ID. The purpose of the link ID is addressed later in this chapter.

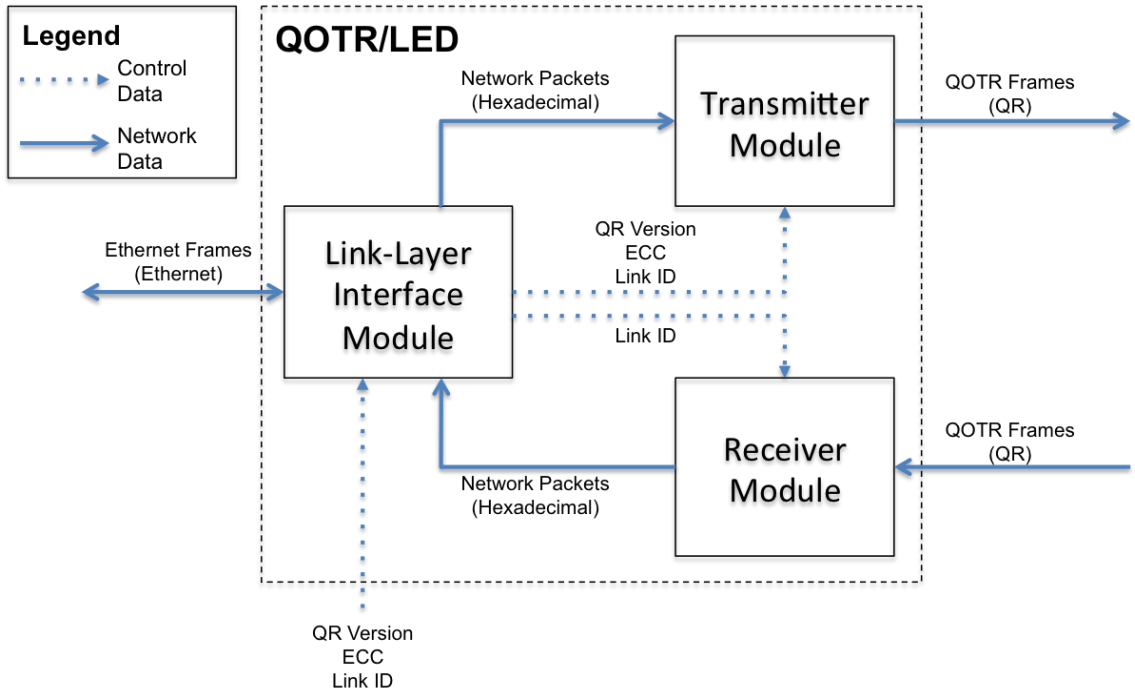

Figure 11. QOTR/LED High-Level Software Architecture.

a. Link-Layer Interface Module

The LLI is responsible for processing and transporting data from the RPi's Ethernet port to the TX and from the RX to the Ethernet port. In addition, the LLI is responsible for conveying all system data and settings throughout all three modules as necessary. The LLI module architecture is shown in Figure 12.

Using the Scapy library, the Ethernet Write and the Ethernet Read processes provide the direct interaction with the RPi Ethernet port. Running in parallel, respectively, the processes output received network packets from the RX Module and read and forward network packets to the TX Module. To allow for buffering of packets between these parallel processes, Python manager shared memory objects were used as queues.

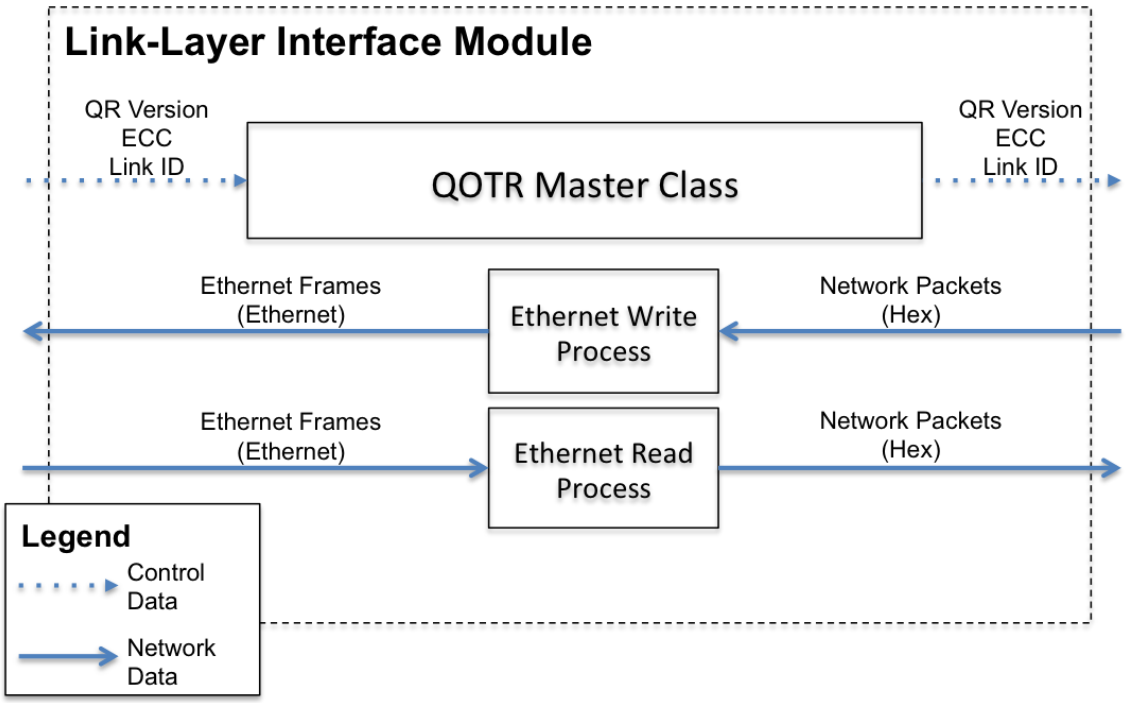

Figure 12. Link-Layer Interface Module Architecture.

b. Transmitter Module

The TX Module processes hexadecimal frames into a series of transmittable QOTR segments and projects them on the LED matrix. A segment is the physical-layer structure used to transmit QR data in the QOTR/LED system. The TX Module is instantiated as a thread from the QOTR Master Class and consists of four separate classes, shown in Figure 13. The TX Module was not able to leverage multiprocessing because Adafruit RGB Matrix objects cannot be passed between processes.

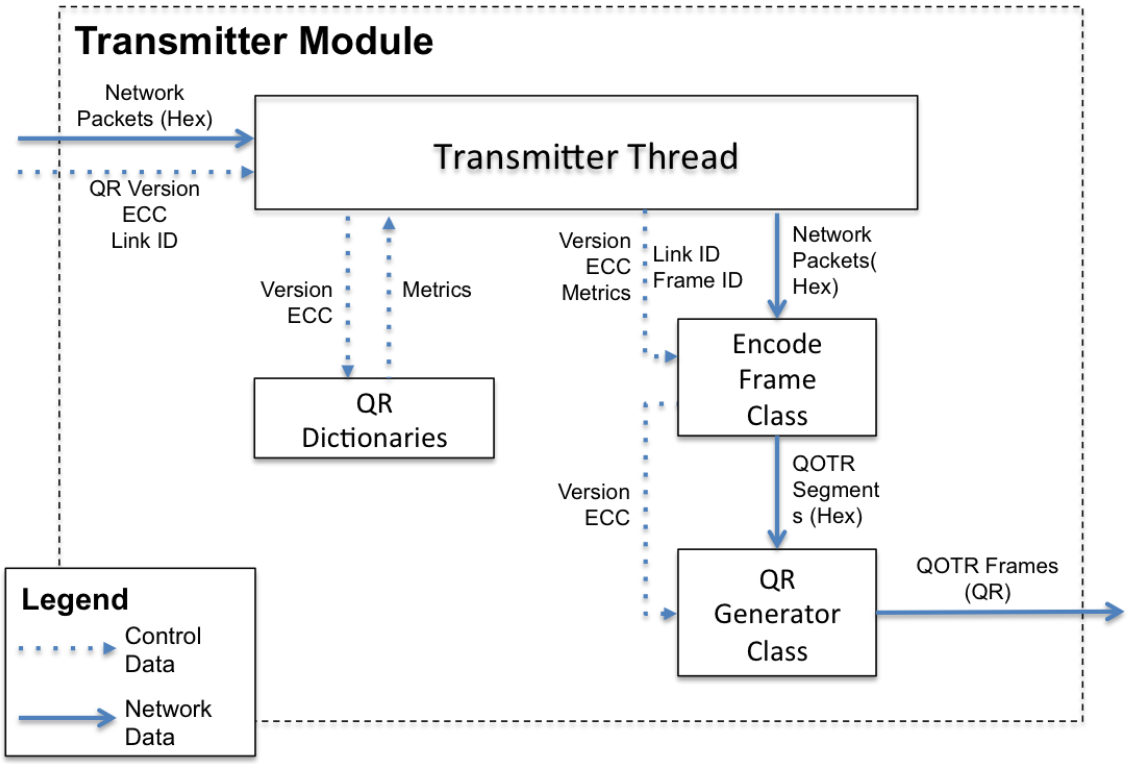

Figure 13. Transmitter Module Architecture.

The overall class in the Transmitter Module is the Transmitter Thread. In addition to receiving raw packets from the LLI Module, the thread also receives control data consisting of the link QR version, ECC, and ID. The Transmitter Thread sends the version and ECC information to the QR Dictionaries file in order to determine the hexadecimal capacity of the chosen QR Code format.

Once the Transmitter Thread receives these QR metrics, it is able to fragment packets in preparation for QOTR segment conversion. In order to differentiate packets, the Transmitter Thread assigns each packet a pseudo-unique Packet ID, ranging from 0 to 255, which is passed with the packet to the subordinate classes in the module. The fragmentation process is shown in Figure 14.

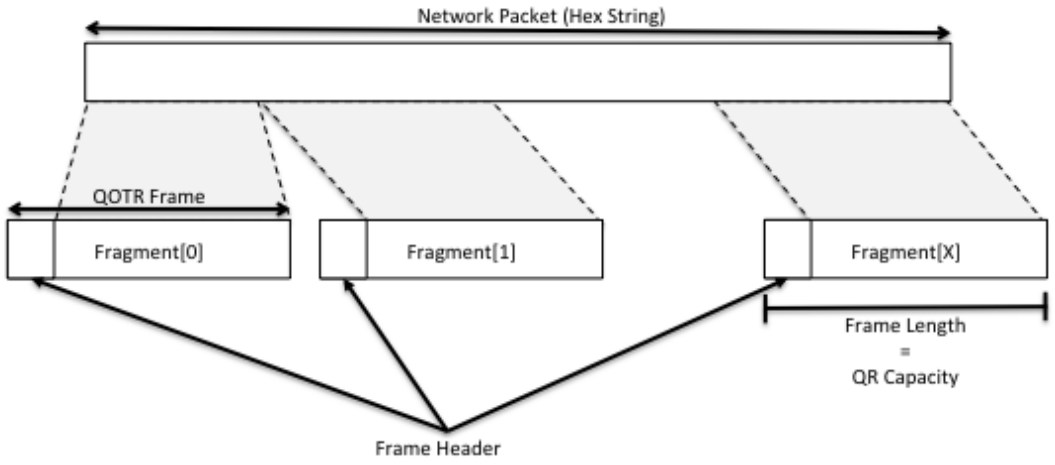

Figure 14. QOTR Fragmentation Process.

Once fragmented, the Transmitter Thread creates an Encode Packet object for the packet, with the packet in the form of a hexadecimal list. The Encode Packet object takes each fragment and places a three-byte QOTR frame header on it, resulting in a completed hexadecimal QOTR frame. The structure of a QOTR frame is discussed later in this chapter. The Encode Packet object then creates a QR Generator object for this segment, which uses the PyQRCode library to build a text mode QR code. It then displays this code on the LED Matrix using the Adafruit Matrix library. The Encode Packet object creates a QR Generator object for every QOTR segment in a frame. Upon completion of transmitting all frames for that packet, the Encode Packet object is deconstructed, and a new object is created for the next packet.

c. Receiver Module

The RX Module is responsible for optically receiving LED QR codes and for recompiling the data into hexadecimal packets. It consists of two classes: the Receiver Process and the Scanner Thread. These two classes run simultaneously; their relationship can be seen in Figure 15. The RX module is instantiated by the LLI Module by calling the Receiver Process, passing it the system's Link ID. The Receiver Process in turn calls the Scanner Thread.

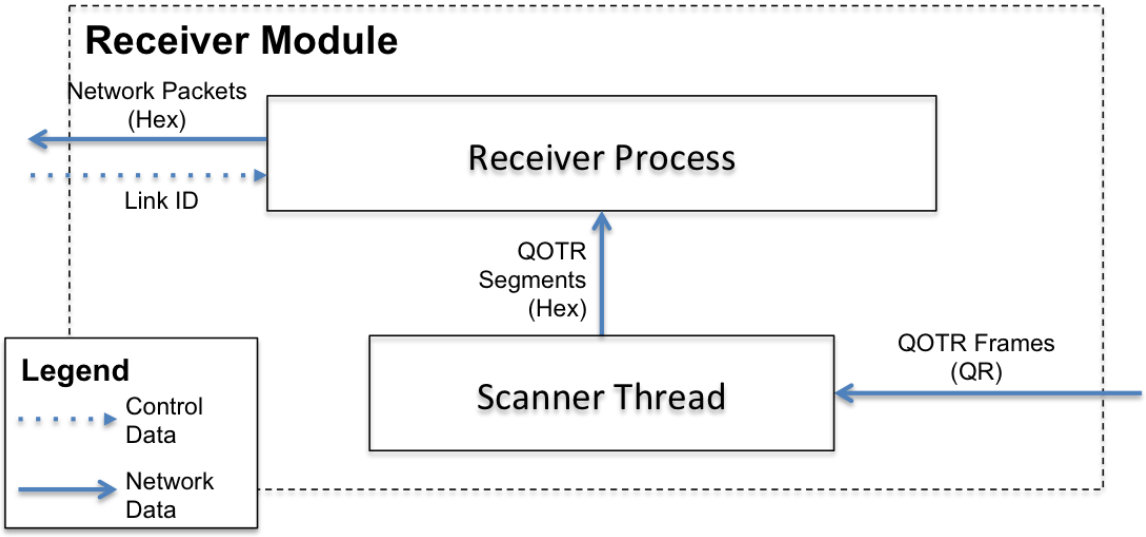

Figure 15. Receiver Module Architecture.

The Scanner Thread is responsible for capturing and processing QR frames from the system's webcam. It does this by using the OpenCV and the Zbar-Python libraries. Using a five-frame buffer, it scans every image for the existence of a QR code. Zbar does the heavy lifting of identifying the version and ECC of the QR code inside the image. The Scanner maintains the most recently decoded frame as a class attribute.

The Receiver Process is responsible for taking hexadecimal QOTR frames and compiling them into their original network packets. Taking the most recent frame from the Scanner Thread's class attribute, the Receiver Process strips off the QOTR frame header and processes it to determine the specific

action to take for the frame. The QOTR frame header composition is discussed in depth later in this chapter. The Receiver Process can take one of three actions with the packet fragment within each QOTR frame: concatenate the fragment with the currently compiling packet, start a new packet with the fragment, or discard the fragment.

The Receiver Process operates at a faster rate than the Scanner Thread; it is possible, therefore, for the Receiver Process to process the same QOTR frame twice, while at the same time preventing the RX from missing any transmitted frame. To prevent the same frame from being added to a packet multiple times, if the hexadecimal string of a frame matches the previous frame, the frame is discarded. Future development of this software will include more advanced timing and synchronization to optimize the interaction between the Scanner and Receiver classes.

3. QOTR Frame

As discussed in Chapter 2, it was necessary to develop a new link layer protocol to support transmission using the QOTR/LED system. This included designing a header for this protocol. After considerations including header length, host addressing, and sequencing, it was decided that a QOTR frame header format of 3 bytes is sufficient. The format includes four elements: terminal bit, link ID, packet ID, and frame ID, as shown in Figure 16.

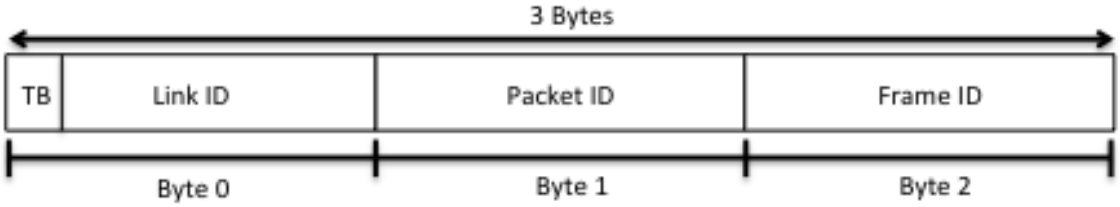

Figure 16. QOTR Frame Header Format.

a. Terminal Bit

The first bit in the header is used to signal whether there are any more frames associated with the current packet. A value of 0 signals there are more frames and a value of 1 signals this is the final frame.

b. Link ID

The Link ID (LID) byte is used to ensure that the QOTR link is operating between the correct Transmitter/Receiver pair. A value between 0 and 127, the LID is set by the user in the LLI Module and is then passed to the TX and RX modules for frame generation and validation. The TX Module attaches the LID to every frame header, taking up seven bits of data. After the frame is received and decoded at the distant RX Module, the LID is compared against the receiver's LID. If they match, the frame continues through the reception process. If they do not match, the frame is discarded.

c. Packet ID

The Packet ID (PID) byte is used to identify to which frame a QOTR segment belongs. The value is a pseudo-unique integer between 0 and 255, which is assigned to a packet by the Transmitter Thread. Processing of the header works similar to the LID. After being included in the transmitted QOTR frame header, the distant RX Module then decodes and compares the PID against the previously received frame. If the receiver is expecting another frame for the current packet and the PIDs match, the frame is retained. If they do not match, the frame is discarded.

d. Frame ID

The Frame ID (FID) is used to ensure that all frames associated with a packet are received in sequence. Due to the nature of the optical transmission channel, frame transmission will only be done in sequence. Therefore, if the Terminal Bit indicates there are more frames to come but the next FID is not the expected value then the entire packet must be discarded.

The FID can have a value of 0 to 255, which limits the total number of frames that a packet can be broken into to 256. Even with the lowest capacity QR code, which, when removing the bytes needed for the frame header, is 8 bytes, this number of frames can still hold more than 1500 bytes of data, the largest size of a TCP packet.

C. ARRAYED-LASER EXPERIMENTATION

The ultimate goal of the QOTR system is to communicate via arrayed laser diodes. This thesis initially sought to conduct analysis of a 3-by-3 laser array in addition to the QOTR/LED system testing. However, due to limitations with the diodes to be tested, this experimentation was not able to be completed.

1. Design

An experiment was designed to test the operation of laser diodes in close proximity by varying the pitch between the diodes in a 3-by-3 array. Consulting the Naval Postgraduate School laser safety officer, it was determined that the tests should be limited to Class II lasers for safety reasons. When combined for testing, the nine diodes would equate to a Class IIIR laser.

The diodes selected for testing were the Quarton VLM-650-03 LPT Laser Modules. They were chosen because they are Class II lasers with minimal beam divergence for their quality. The specifications for these diodes are shown in Figure 17. 3-by-3 mounts were created with 3-dimensional (3D) printing to ensure that the diodes were mounted in parallel. The 3D printer's tolerance was 0.002 mm. The entire system was driven by an Arduino Mega 2560 board [30].

SPECIFICATIONS

	SPECIFICATIONS	635-03	650-03
1	Dimensions	Φ7 x 21 mm (Φ0.276" x 0.827")	
2	Operating voltage (Vop)	2.6~5 VDC	
3	Operating current (Iop)	< 50mA	< 35mA
4	Continuous wave output power (Po)	LPT<1mW / LPA≦2.5mW	
5	Wavelength at peak emission (λp)	630~645nm	645~665nm
6	Collimating lens	Aspherical plastic lens(ø5)	
7	Spot size at 5M	6±1 mm	
8	Divergence (Half Angle)	0.6 mRad	
9	Operating temp. range	+15°C ~ +30°C (Room Temperature)	
10	Storage temp. range	-20°C ~+65°C	
11	Housing	Steel	
12	Mean time to failure (MTTF) 25℃	5000hrs	10000hrs

Figure 17. Quarton VLM-650-03 LPT Laser Module Specifications. Source: [31].

2. Shortfall

Upon mounting the laser diodes in the 3D printed mounts, it was found that the diodes were not projecting in parallel. While it had been predicted that the challenge in achieving parallel beams would originate from the mount itself, but upon further analysis it was found that the actual diodes did not project at identical angles to one another. This is likely because of low tolerances in the manufacturing process. Because of this, it was not possible to accurately test the system.

Additionally, as is true with most individual laser diodes, the beams for the Quarton VLM-650-03 LPT laser modules were elliptical, not circular. This means that for proper arrayed transmission the diodes would not only need to be aligned in parallel but also rotated to the same orientation.

3. Summary

Achieving a properly arrayed MIMO setup of laser diodes proved to be extremely difficult and unattainable for this thesis. Future implementation of should consider higher quality laser diodes or possibly VCSELs, which are manufactured in parallel. VCSELs have the added benefit of being circular beams [17].

D. QOTR EXPERIMENTATION

Chapter 4, “Testing and Analysis,” reports the results of the experimentation accomplished on the QOTR/LED system, which was focused on evaluating the resilience and scalability of the QOTR link layer protocol. Analyzing the performance of the system included the measuring of three different metrics: data rate, range, and error correction performance. The system described in this chapter depicts a full duplex system; however, for testing a simplex system was used in order to analyze the performance of a single optical channel. Due to the use of LEDs instead of laser diodes, range and viewing angle were not metrics studied in this thesis. Future implementations of the QOTR system should consider these attributes.

THIS PAGE INTENTIONALLY LEFT BLANK

IV. TESTING AND ANALYSIS

This chapter presents the experimentation results and analysis for the testing of the QOTR/LED system outlined in Chapter 3, “System Design.” Testing of the QOTR/LED system was conducted in a laboratory environment. A simplex system consisting of a single LED transmitter and single optical receiver was used in order to validate the implementation of the QOTR link layer protocol.

A. EQUIPMENT SETUP

For the laboratory testing, multiple changes were made to the hardware architecture outlined in Chapter 3 in order to adapt the system to simplex testing. However, the underlying Python modules remained the same. In addition to the receiver and transmitter, an RPi was connected to the transmitter via Ethernet cable to pass randomly generated network traffic for transmission. The entire equipment string was set up in a bench top configuration, as shown in Figure 18.

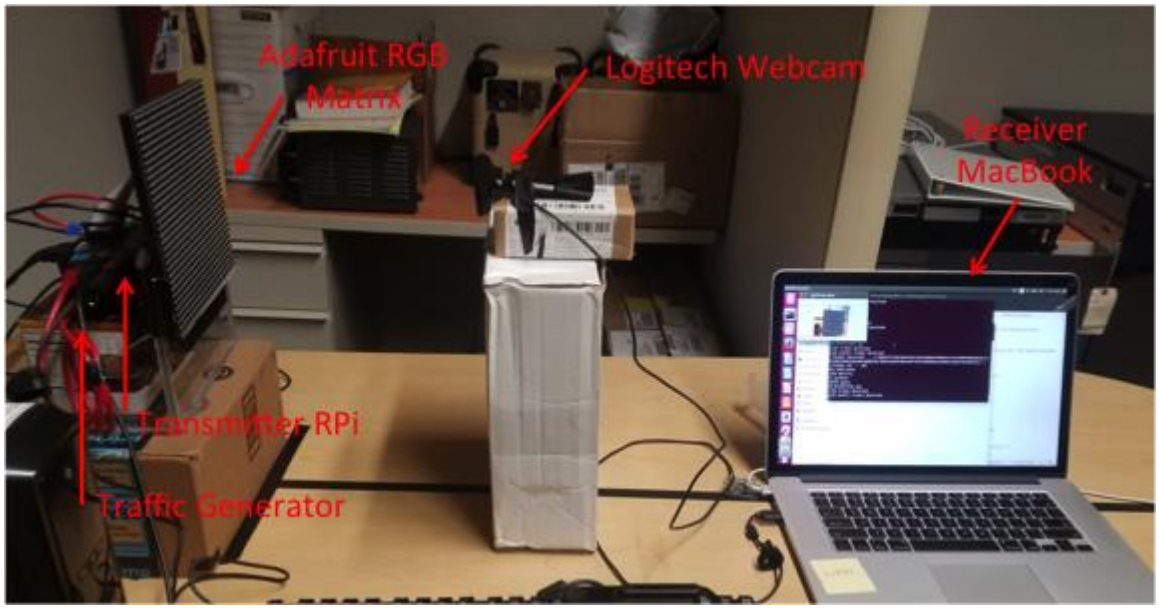

Figure 18. Bench-top QOTR/LED System Setup.

1. Traffic Generation

Initial traffic generation for testing was done using randomly created packets from an RPi 3, including DNS, ICMP, and HTTP packets. However, these packets lacked the robustness of typical network traffic and failed to effectively test the QOTR link layer protocol. Typical traffic generators, such as Cisco's T-Rex were designed to test much larger bandwidth pipes and ended up overwhelming the QOTR/LED system's limited bandwidth.

After exhausting these initial solutions, packet generation was done by selecting random packets from a PCAP (Packet capture) file logged from a laptop on the NPS wireless LAN. The EthernetRead module was set up to not forward ARP frames that were also present on the Ethernet link between the QOTR system and RPI traffic generator. This PCAP contained over 3000 packets, ranging in size from 40 to 3990 bytes in length. This more accurately represented the kind of traffic that would be transmitted across a QOTR/LED link and better stressed the QOTR protocol.

2. Transmitter

The transmitter hardware for the simplex QOTR/LED test did not change from the presented system design. It consists of an RPi 3, RPi HAT, and an Adafruit 32x32 LED board.

3. Receiver

The major change to the simplex equipment string was replacing the receiver RPi with a more powerful, MacBook Pro CPU. The receiver webcam was placed 1 foot from the transmitter in order to establish the optical link. During link calibration, it was found that capturing the OpenCV frames at the webcam's standard resolution of 1080 by 720 pixels made it extremely difficult for the Zbar library to recognize the LED QR codes. After trial and error, it was found that the optimal resolution for QR recognition was 240 by 180 pixels. This resolution provided enough granularity to clearly recognize the QR pixels, while at the same

time was not so clear as to cause the camera's auto focus to overcompensate for the rapidly changing images.

B. OPTICAL LINK TESTING

Testing of the optical channel was conducted in five-minute intervals. This was due to the performance of the Adafruit LED board operating on the RPi HAT, which occasionally caused the RPi 3 CPU to crash after sustained QR code transmission. It is suspected that this is due to the CPU overheating when driving the matrix for long periods of time. Proposed solutions to this issue are addressed at the end of this chapter.

Testing was conducted for all four ECC levels of the Version 3 QR format, consisting of 29-by-29 pixel images. The QR version was selected because it was the largest size that the 32-by-32 Adafruit LED matrixes could support. Each ECC was tested for ten, five-minute trials, resulting in a total of 40 trials for the entire experiment. Table 2 shows the capacities of each Version 3 ECC level and the associated byte capacity after removing the three bytes required for the QOTR frame header. Even with the low ECC, every network packet transmitted required at least two frames in order to be transmitted considering the minimum packet size is 40 bytes.

Table 2 QOTR Protocol Capacities by ECC Level.

	Alphanumeric Characters	W/O Header	Byte Capacity
L	77	71	35.5
M	61	55	27.5
Q	47	41	20.5
H	35	29	14.5

1. Results

Table 3 shows the summarized results for the four ECC level test scenarios. The values shown are the average of all ten trials. The complete test results can be found in “Appendix D: QOTR/LED Experimentation RESULTS.”

Table 3 Summary of QOTR/LED Testing Results.

	Avg Frame Rate (fps)	Avg Transmission Rate (bps)	Avg Throughput (bps)	Frame Usage	Bit Error Rate	Packet Error Rate	Frame Error Rate
L	3.73	1035.22	933.20	97.81%	9.84%	4.60%	0.25%
M	3.71	797.21	787.26	97.78%	1.26%	0.74%	0.03%
Q	3.55	569.71	569.71	97.93%	0.00%	0.00%	0.00%
H	3.57	408.50	408.50	98.64%	0.00%	0.00%	0.00%

In this table, four additional metrics were calculated to assist with analysis. The frame error rate (FER) is the average QR frame loss percentage for the link. The packet error rate (PER) is the average packet loss percentage for the link. The byte error rate (BER) is the average byte loss percentage for the link. Lastly, the frame usage is the percentage of all QR code data capacity used to carry network packets. Frame Usage was calculated using the following formula. *Bytes* is the number of bytes actually transmitted, N_f is the number of frames transmitted, and *Cap* is the byte payload capacity of the QR version.

$$Frame\ Usage = \frac{Bytes}{N_f * Cap}$$

The Low ECC scenario experienced the greatest loss of all the test cases. Despite only losing one in every four hundred QR frames, this still translated to a BER of nearly 10%. While the Medium ECC test case was more efficient, it still demonstrated that the loss of just a few QR frames can result in a relatively large negative effect on the BER. The Quartile and High ECC test cases proved more

successful, observing no frame losses across all tests. This supports the hypothesis that the use of the QR format's inherent error correction can aid in overcoming deficiencies in optical links.

As the ECC level increased from Low to High, there were multiple trends observed. As expected, as the error correction percentage increased, the transmission rate decreased. Additionally, with the ECC increase the Frame Usage also increased. An interesting characteristic that was observed was the lower average frame rate of the Quartile and High tests compared to the Low and Medium tests. Throughout the testing, no additional code was added to the EncodeFrame or QRGenerator classes, which is why one would expect to see slower frame rates. This implies that there is a difference in the coding overhead required to encode packets with Quartile and High ECC. With the limited number of trials conducted, this phenomenon should be studied more in future work.

2. Analysis

While the QOTR/LED system testing validated the implementation of the QOTR link layer protocol designed in this thesis, further analysis reveals the strength and weaknesses of the designed protocol. Analysis was conducted in three areas: the efficiency of the QOTR protocol, the efficiency of the QOTR/LED transmission system, and extrapolating the results to project the efficiency of large-scale QOTR employment.

a. Efficiency of the QOTR Protocol

This section addresses the efficiency of the QOTR link-layer protocol. It considers the characteristics of converting packets into a series of QR codes and does not address whether these QR codes are transmitted successfully or not.

The major metric that characterizes the efficiency of the QOTR protocol is Frame Usage. The two parameters that intuitively would have an effect on this metric are the ECC level and the size of the packet being encoded. Figure 19 shows the plot of these parameters against the observed frame usage. While

there does appear to be a direct relationship between Frame Usage and both the ECC level and average packet size, this relationship is very subtle. The High ECC level does cause a more distinct increase from the Quartile ECC level. However, this difference still only results in the 0.71% increase in usage.

The relationship between average packet size and Frame Usage is even less defined, and because this is a parameter that is extremely difficult to control on a network, it can be concluded that it will not be a consideration in selecting link parameters. Overall, while ECC level does have an effect on frame usage, this effect is low and implies that frame usage alone should not be used as a decision point for what ECC level to choose.

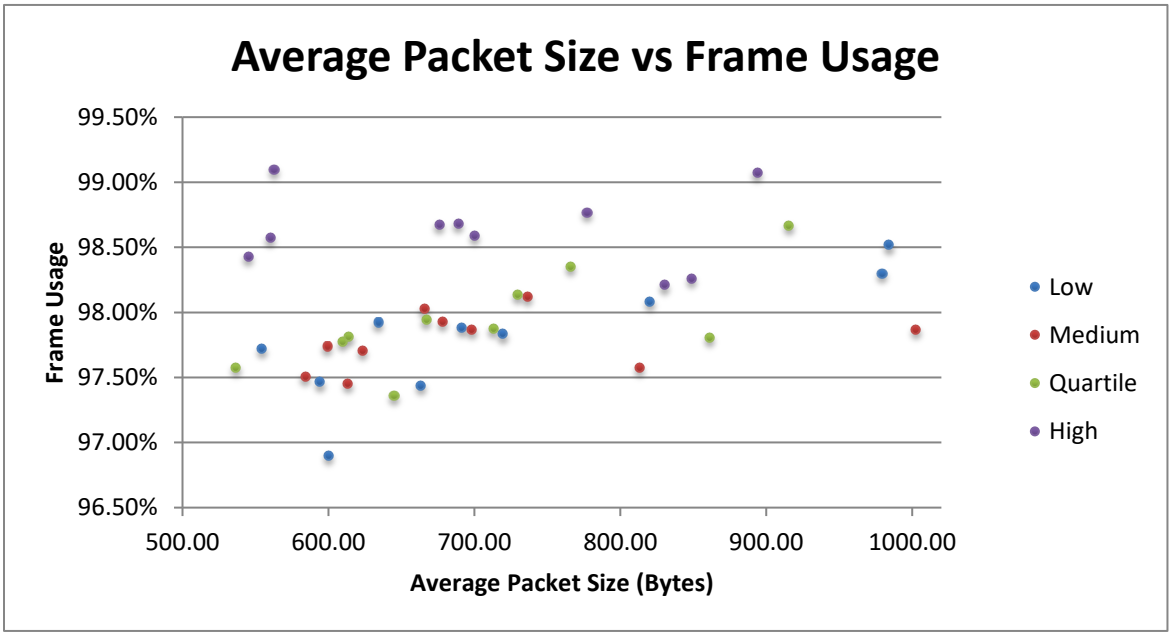

Figure 19. QOTR Frame Usage Analysis.

Frame usage below 100% exists in the QOTR protocol because the protocol only allows one packet to use each QOTR frame. To enable a QOTR frame to hold pieces of two different packets would require more robust header information, which would reduce the payload capacity of the frame. However, it

would eliminate the padding that is often added to the final frame of a packet in the current format, resulting in 100% Frame Usage.

To evaluate if this is a viable change to the current QOTR format, it will be assumed that the header will have to double in size to six bytes. For evaluation purposes, the current format will be estimated to have a Frame Usage of 95%, which is generous according to our tests. Table 4 shows the comparison between these two header formats. For QR Version 3 it appears that the current version of the header is more efficient even considering the 95% frame usage. However, as the overall capacity of the frames grew, a format that accommodates two packets using the same frame begins to be more efficient, despite the increased header length. It should also be noted that in our tests we witnessed the frame usage decrease as capacity grew, so with larger codes the actual usage might drop below 95%. Because of this, future evaluation of the QOTR protocol should include testing of larger QR versions in order to characterize this further.

Table 4 QOTR Header Format Comparison

QR Version	ECC	Capacity w/ Byte Header (95% Usage)	Capacity w/ Byte Header (100% Usage)
3	*High*	13.78	11.50
	Quartile	19.48	17.50
	Medium	26.13	24.50
	Low	33.73	32.50
5	*High*	27.55	26.00
	Quartile	38.48	37.50
	Medium	55.10	55.00
	Low	70.30	71.00
6	*High*	37.05	36.00
	Quartile	48.45	48.00
	Medium	70.30	71.00
	Low	89.78	91.50

b. Efficiency of Transmission

This section addresses the efficiency of the optical link established in the QOTR/LED system. Figure 20 and Figure 21 show plots of the measured transmission frame rate against the link transmission rate and the link throughput, respectively. There appears to be a somewhat linear relationship between the four ECC levels and their respective transmission rates. Of note, it also appears that more error correction also translates to slower transmitter frame rates. This is likely explained by a need for more coding overhead to accomplish the more robust error correction. However, the overall difference in frame rates is relatively small, with all trials falling between 3.46 and 3.83 frames per second.

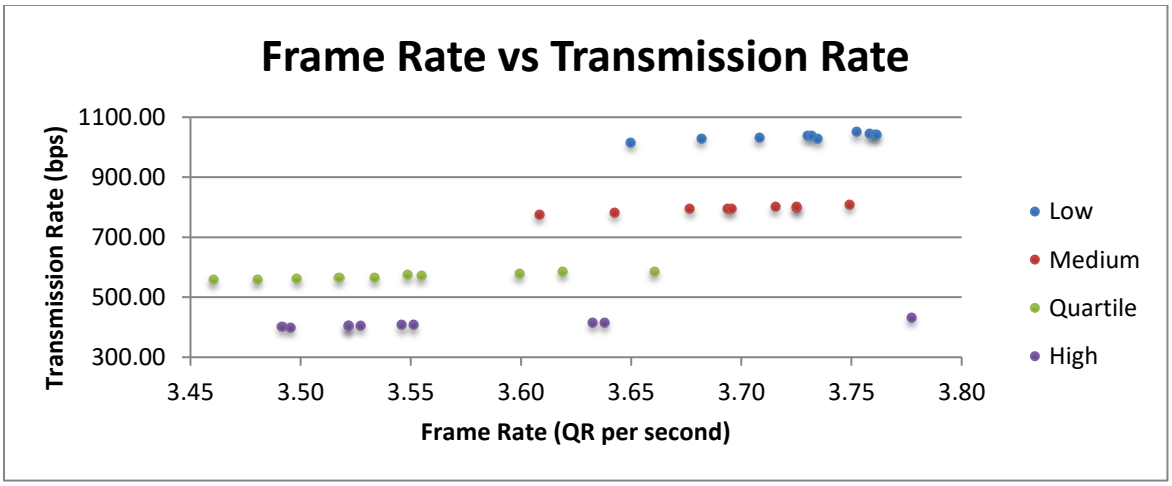

Figure 20. Frame Rate versus Transmission Rate Plot.

Figure 21 illustrates the error that was incurred in QOTR links with lower error correction. While all trials in the Quartile and High ECC levels experienced no frame loss, resulting in identical transmission rate and throughput values, trials in the Medium and Low ECC level tests did experience errors. Three trials in the Medium tests all dropped one frame each and eight trials in the Low tests dropped frames, ranging from one to six frames. Frame loss in these links was likely caused by optical interference caused as the Adafruit LED matrix diodes' rapid changes, causing glare. While reducing the resolution of the Logitech webcam helped mitigate most of these errors, they still exist when using low ECC settings. A higher quality camera that gives the user more control over shutter speed, exposure rate, and focus settings would likely be able to provide better image quality to reduce the frame loss of the Low and Medium ECC level links to near zero.

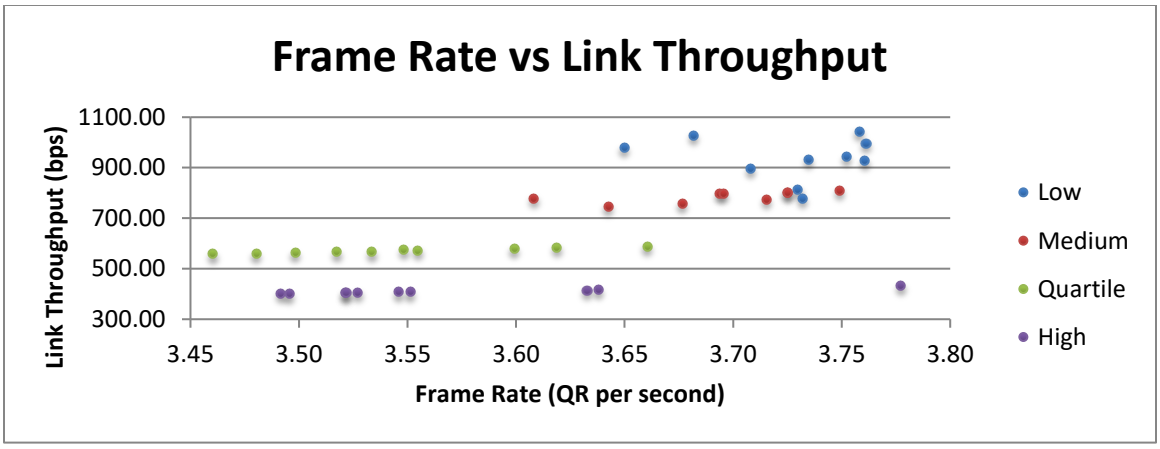

Figure 21. Frame Rate versus Link Throughput Plot.

To better understand the effect of frame loss on the PER and BER, the eleven trials that experienced frame loss have been studied further. By comparing FER with PER, Figure 22 shows a clear exponential relationship between the two metrics, with the PER increasing more sharply as FER increases. This reflects how the QOTR protocol works. While there is error correction at the receiver for each individual frame, there is no error correction for packets. If one frame is lost in a packet, then the entire packet is discarded, making other packets that were successfully received unusable. From the data collected, an R^2 value of 94% was associated with this exponential relationship. However, more testing should be conducted to confirm and refine the relationship.

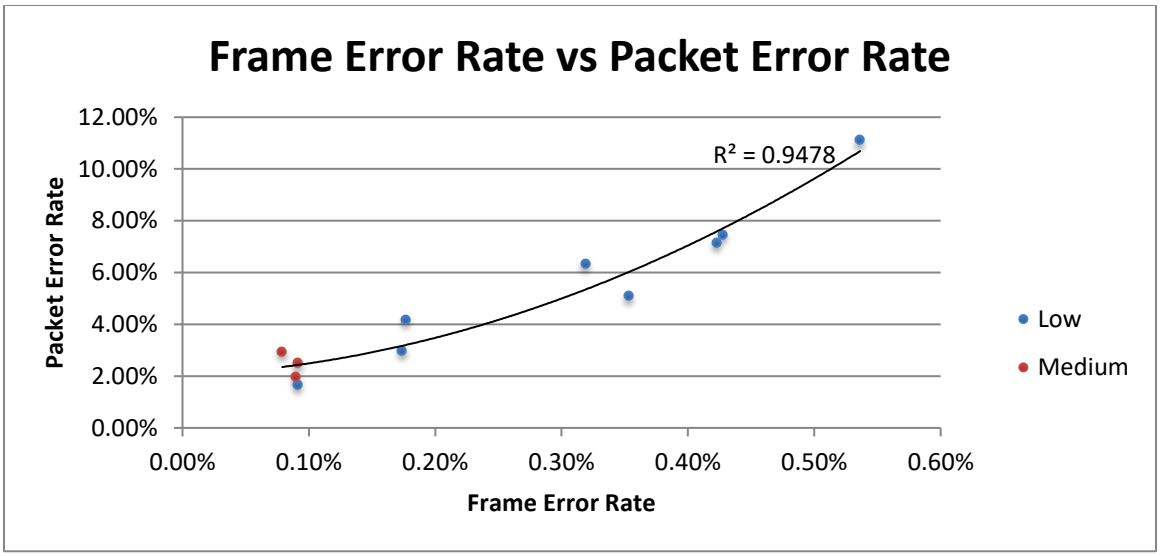

Figure 22. Analysis of FER on PER.

The relationship between FER and BER was less distinct. Figure 23 depicts the relationship between these metrics. Even more than PER, BER increases sharply with more frame loss. This is to be expected. Since the loss of a single frame results in the loss of an entire frame with the current structure of the QOTR protocol, it is more likely that the packet will have a larger number of bytes since larger packets have more frames than can be lost. In testing, this was most pronounced in the Low ECC level trials, where one trial that lost only one in 300 frames resulted in the loss of 25% of its throughput.

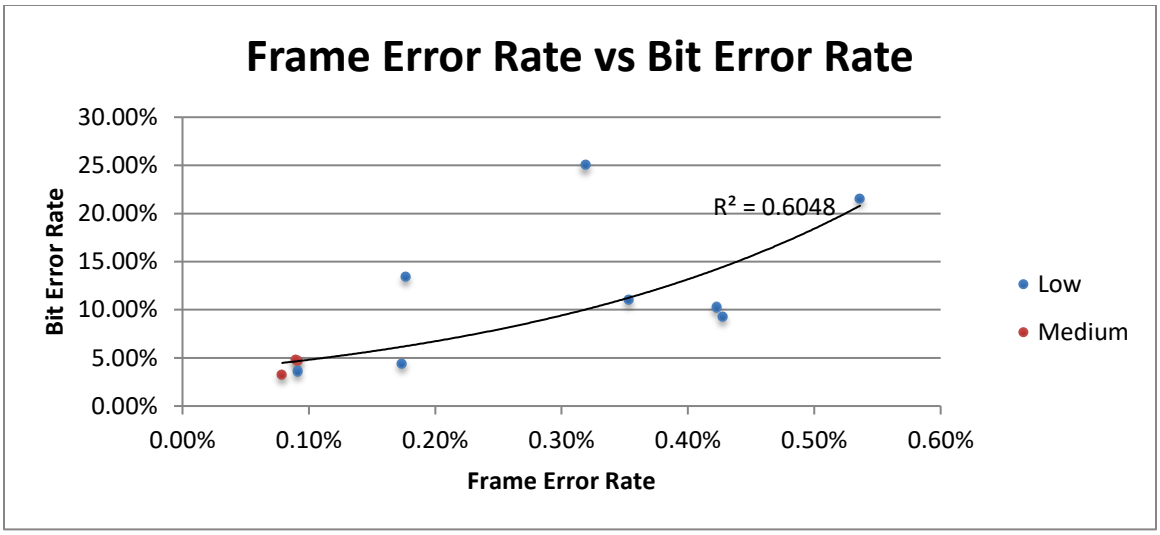

Figure 23. Analysis of FER on BER.

The exponential relationship between frame loss and PER and BER is one of the largest issues with the QOTR protocol that was discovered during this testing. While the fragmenting of packets to fit in QOTR frames is similar to IP fragmenting used in the network layer, the QOTR fragmenting requires the packet to be reconstructed in stream as opposed to IP fragmenting which is conducted at the destination node. This is not a viable solution for the QOTR protocol since the size of fragments can be extremely small, as low as 14 bytes in our testing scenarios. A possible solution for this issue that maintains the current format of the QOTR protocol is the use of forward error correction (FEC) on network packets prior to QOTR fragmenting. While this would increase the payload of each packet, it would also increase link stability, likely making the use of Low ECC levels more viable.

c. Extrapolation for Large Scale Use

The ultimate goal of developing the QOTR system is to study the feasibility of developing a MIMO FSO system that operates using laser diodes. As discussed in Chapter 2, “Background,” laser diodes have been proven to transmit in excess of multiple Gbps data rates, however, high speed camera technology is typically limited to the million frames per second range with the current state-of-the-art devices. Because of this, in extrapolating the results of this experiment to predict the metrics of a more robust QOTR system, we will focus on the limiting factor, receiver frame rate.

Testing of the QOTR system demonstrated that lower camera resolutions were preferable to higher resolutions when attempting to read QR images. The final camera resolution used for the QOTR system was 240-by-180 pixels. Understanding that current ultra high-speed cameras are capable of recoding approximately 100 thousand FPS, we extrapolated the results of the QOTR/LED system tests in order to predict the throughput of a QOTR link utilizing this type of receiver. This extrapolation is shown in Figure 24 reflecting all four ECC levels for QR version 3.

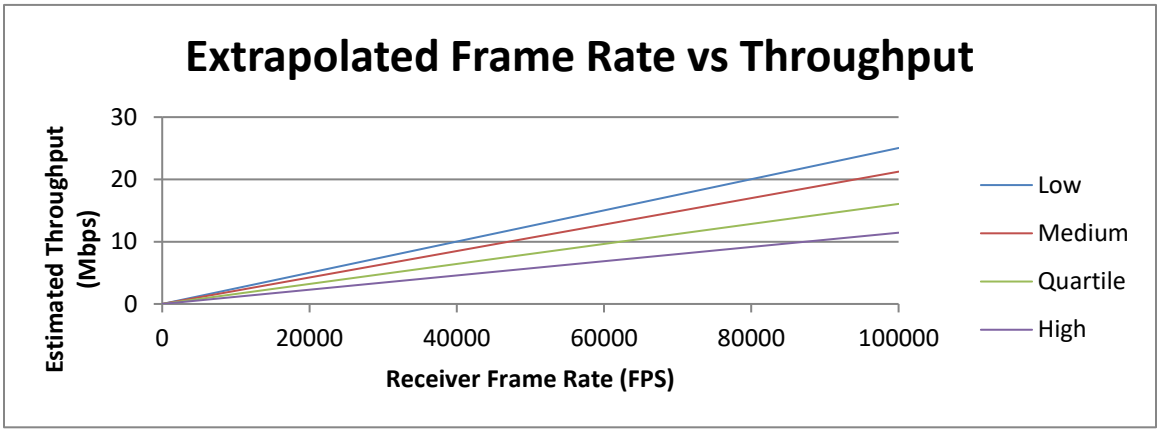

Figure 24. Extrapolation of QOTR/LED Testing Results.

The maximum theoretical throughput reached with this setup is 25 Mbps. While this is competitive with current tactical multi-channel radio data rates, it is

substantially less than the current benchmark in tactical FSO systems, set by the TALON system with a 1 Gbps link [11]. To reach a link throughput in this range while maintaining this frame rate the QR format must be increased from Version 3 L to Version 29 L, which is a 133-by-133 array [7]. Given current laser diode technology, this is unrealistic.

The limitation of this extrapolation is that it does not take into account the CPU power and memory required to process the millions of QR images being received. Current high-speed cameras contain hundreds of GBs of RAM to cache the images received. The iX i-SPEED 7 camera can contain up to 288 GBs of RAM, and even with that it is only able to store 8.5 seconds worth of frames at 1064-by-228 pixels [18]. Coupling this type of camera with the QOTR system would require a high-speed, multi-core CPU to ensure that the QOTR frames received could be processed faster than the camera could cache them.

C. SUMMARY

Testing of the QOTR/LED system was successful in demonstrating the concept of MIMO FSO transmission using QR codes and the viability of the QOTR link layer protocol. While the system achieved limited throughput capability, averaging less the 1 Kbps, the low FER observed validates the theory that the inherent error correction of QR encoding is valuable in MIMO FSO transmission.

With frame usage above 95% during all testing trials, the current structure of the QOTR frame header has been found to be the most efficient means in linking frames, despite its lightweight characteristics. However, if the QOTR system is scaled to accommodate larger QR formats testing should be done to determine if a more robust header format that supports the transmission of fragments of multiple packets in the same frame is more efficient.

The requirement of the QOTR protocol to reassemble fragmented packets at the receiver node proved to be the source of the most error in the system. While a link's FER may be low, this can result in a disproportionate PER and

BER depending on the size of the packets to which lost frames belong to. A simple solution to this issue may be to implement FEC on packets before they are processed into QOTR frames.

Finally, in studying the feasibility of scaling the QOTR system using current commercial equipment it was found that the limiting factor is the current capabilities of high speed imaging equipment. Current camera frame-rate capabilities only support MIMO FSO communications using QR encoding in the Mbps data rate range with the test QR versions. Further research should be done to study the viability of using larger QR versions to achieve data rates that are more comparable to the Gbps links achieved by SISO FSO systems.

THIS PAGE INTENTIONALLY LEFT BLANK

V. CONCLUSION

This chapter provides a conclusion with respect to the stated objectives from the first chapter. Potential future work following this thesis is also discussed.

A. OBSERVATIONS

This thesis was successful in achieving its three key goals of understanding MIMO FSO, designing a MIMO FSO system using COTS equipment, and designing and executing experiments to evaluate the performance of the designed system.

Nearly all FSO systems in use by the military and civilian sectors utilize SISO system architectures. MIMO FSO has not been extensively studied for long distance implementation, instead being mainly used in laboratory environments. Adapting MIMO FSO systems to operate over longer distances, in outdoor environments, as part of large-scale communications networks would likely enable new types of FSO link architectures and possibly provide larger bandwidth connections. Additionally, they can overcome some of the loss associated with SISO FSO links because of the optical error correction techniques that can be used. However, implementing large-scale MIMO FSO requires overcoming various technical challenges with regard to the transmitter and receiver hardware employed and the operation of multiple optical diodes when arrayed in close proximity, to include challenges with aligning the optical beams.

The QOTR/LED system was developed to study the performance of a MIMO FSO that uses optical QR codes for transmission. The transmitter was constructed of an RPi 3, RPi HAT, and Adafruit LED Matrix while the receiver required higher processing power from a MacBook Pro combined with a Logitech webcam. Coding for the entire system was done in the Python 2.7 programming language. The QOTR/LED system used the QOTR link layer protocol to transmit network packets. Looking to the 802.3 Ethernet and 802.11 WiFi protocols for

inspiration, the format of the QOTR protocol was designed with the following qualities in mind: unique addressing, minimal header size, and proper QR code sequencing.

The QOTR/LED system successfully transferred data over an optical simplex link using randomly generated network traffic. The achieved data rates were limited to 1 Kbps due to the frame rate of the Adafruit LED Matrix working in conjunction with the RPi 3, which could only reach approximately 3.75 FPS. For all tests, the QR code version was kept constant at Version 3, while the error correction level was varied between Low, Medium, Quartile, and High. Despite the low data rates achieved, we were able to analyze the QOTR/LED system and the QOTR link layer performance, resulting in three major observations.

1. The QOTR Header Format is Effective

Due to an average frame usage of 95%, the current QOTR header is the optimal choice for QR code Version 3 transmission, but larger QR code versions could see better performance with a larger, more dynamic header format.

2. QOTR Frame Loss Causes Disproportionate Packet and Bit Loss

The most significant inefficiency with the QOTR protocol was the result of the disproportionate affect the frame error rate can have on packet and bit errors rates. This may be able to be solved by using forward error correction in the future.

3. The Theoretical Bandwidth of QOTR System is Comparable to SISO System

By extrapolating the QOTR/LED's performance with known hardware capabilities, the theoretical data rate of a large-scale QOTR system is comparable to current SISO FSO systems. Due to this, the advantages of QOTR systems over SISO employment with current state-of-the-art are limited to providing image inherent error correction and the possibility of creating unique

network architectures. However, there may be other types of MIMO FSO systems that provide superior bandwidth performance than SISO FSO systems. FSO utilizing multiple optical wavelengths in parallel is a possible area of further research.

B. SUMMARY

While the QOTR/LED system proved successful in implementation, it was found to not possess as many advantages over SISO FSO systems as initially expected. Additionally, in attempting to test the operation of laser diodes in parallel it was found that this seemingly simple task requires a minute level of calibration to successfully implement. Therefore, scaling the QOTR system from using LEDs for the optical channel to using laser diodes will take high quality manufacturing and workmanship. The QOTR/LED system provides a blueprint for the construction of such a system and demonstrates the vital concept of chaining optical QR codes to transmit network data.

With further research, MIMO FSO appears to be an advantageous communications method for tactical communications, with the most valuable quality being possible employment topologies. The Indirect Line-of-Sight (ILOS) and MIMO Broadcast topologies proposed in “Appendix C. Concepts of Employment” offer unique network architectures for tactical scenarios. Continued development of the QOTR/LED system should seek to leverage these topologies.

C. POTENTIAL FUTURE WORK

The concepts behind the QOTR/LED system offer great potential for tactical employment. The following are various lines of effort that will further develop the QOTR and the QOTR protocol.

1. Further Development of QOTR/LED System

The QOTR/LED system needs to be further developed to support both full duplex operation and higher frame rates at the transmitting node. The current

limitations in achieving this are the RPI 3, which does not have the computing power to support more rapid QR frame processing or running the Receiver Module python script. A new computing platform must be selected that has far more robust computing power in order to enable the parallel running of the Transmitter and Receiver Modules as well as high speed driving of the Adafruit LED Matrix. To do so will require the development of the Adafruit RGB Matrix Python library and LED Matrix hardware to interface with an operating system other than the RPI 3. Advances to the receiver imager will also be necessary to accommodate frame rates in excess of 1000 FPS.

2. Arrayed-Laser Experimentation

This thesis' 3-by-3 laser diode testing should be revisited using more advanced laser diodes with the purpose of characterizing arrayed-diode performance. Testing should study the range at which beam divergence makes individual beams indistinguishable between one another. Possible parameters to vary include pitch between diodes, incident angle of diodes, and power output. While starting with Class II and Class IIIR lasers is recommended for cost and safety purposes, the ultimate goal should be to conduct the testing using multiple Class IM lasers in order to best reflect telecommunications technology.

3. Machine Learning Interference Correction

Building upon arrayed-laser experimentation, the use of machine learning may offer a solution to the optical interference caused by beam divergence. Using a machine-learning database of know optical distortions of a certain image pattern, it is theoretically possible to determine the original pattern sent by the transmitter. This concept should first be tested on smaller diode arrays and image databases (3-by-3) and increased to accommodate diode arrays of various QR code dimensions. Studies should be conducted at various ranges to determine the effect of distance on the usability of machine learning databases.

4. Optimized QR Format for Optical Transmission

"Appendix B. QR Encoding," the format of the QR codes used in the QOTR/LED system was designed for individual use. A large amount of the data in this format is used for image alignment and orientation information. Because the QOTR protocol utilizes QR codes in rapid succession, some of this data is redundant when used in the QOTR/LED system and takes away image capacity that could be better used to transmit useful payload data. Research should be done to develop a QR-style image format that is tailored for use in the QOTR FSO system, increasing bandwidth compared to current QR formats by reducing the amount of signaling data in each image.

5. Indirect Line-of-sight Testing and Development

One of the advantages of MIMO FSO over SISO FSO is its ability to be employed in unique network architectures, specifically ILOS and broadcast. The topologies leverage projecting MIMO images upon intermediate objects to create network links between two or more nodes and are further described in "Appendix C. Concepts of Employment." Currently, the topologies are still at the proposal stage and have not been tested with a MIMO FSO system. Research should be done leveraging the QOTR/LED system to validate the soundness of these topologies and assess their capabilities and limitations.

THIS PAGE INTENTIONALLY LEFT BLANK

APPENDIX A. SURVEY OF TACTICAL FSO SYSTEMS

Table 5 Summary of Major Tactical FSO Systems.

System/Experiment	Developer	Year	Data Rate	Conditions
Trident Warrior 2006	Naval Research Laboratory (Novasol, Inc. transmission systems)	2006	300 Mbps at up to 17.5 km	Vessel based, 150 ft above waterline
Free Space Optical Experimental Network Experiment (FOENIX)	Defense Advanced Research Projects Agency	2010-2012	10.3 Gbps at 200 km	Air-to-air and air-to-ground
LaserFire V3	Naval Postgraduate School (in conjunction with SPAWAR and SpacePhotonics, Inc.)	2014	300 Mbps at up to 1.35 km	Ground based
NEXUS 3	Naval Postgraduate School (SA Photonics transmission systems)	2016	4.89 Gbps at 9 km	Ground based
Tactical Line-of-Sight Optical Network (TALON)	Naval Research Laboratory	2017	880 Mbps at 16 km 214 Mbps at 50 km	Ground based, mast up to 110 ft

A. TRIDENT WARRIOR 2006 (TW06)

TW06 involved one of the first major maritime tests of FSO for naval operations. NRL worked with Novasol, Inc. to test various ship-to-ship systems during the transit of the USS *Bonhomme Richard* and USS *Denver* between San Diego, CA, and Honolulu, HI. The constant movement caused by being afloat introduced a new challenge in the alignment of the FSO terminals. During experimentation, a link was maintained passing 300 Mbps digital video at ranges

of up to 17.5 km [9]. Figure 25 shows the NRL FSO terminal mounted above the flight deck of the USS *Bonhomme Richard*.

Figure 25. FSO Terminal on USS *Bonhomme Richard*. Source: [9].

B. FREE SPACE OPTICAL EXPERIMENTAL NETWORK EXPERIMENT (FOENIX)

The Defense Advanced Research Projects Agency (DARPA) teamed with NRL and the Air Force Research Laboratory (AFRL) to experiment with various FSO air and ground systems from 2010 to 2012 during the FOENIX experiment. The experiment was successful in validating air-to-air and air-to-ground FSO links as well as conducting FSO/RF hybrid transmission systems in similar configurations [32]. The highlight of the experiment was the establishment of a 200-mile air-to-ground link at 10.3 Gbps [11].

C. LASERFIRE V3

The LaserFire V3 FSO terminal (Figure 26) is a production grade FSO system built by Space Photonics, Inc., that was initially designed for use in commercial short-distance building-to-building communication with a stated range of 5 kilometers [33]. In 2014, Space Photonics partnered with Naval Postgraduate School and Space and Naval Warfare Systems Command

(SPAWAR) to test the use of the LaserFire V3 system for tactical communications. Testing was done aboard Camp Roberts during Joint Interagency Field Exercise (JIFX) 14-4.

Figure 26. LaserFire V3 Unit. Source: [33].

Testing revealed that the LaserFire system did not possess the qualities to make it ready for deployment in a tactical environment. Specifically, issues were discovered with the range and data-rate limitations of the system. The range of the system tested was 1.35 kilometers, far short of the advertised range and tactical requirements as it was dramatically impacted by ground-effect scintillations. Lastly, the system did not enable it to operate at a reduced data-rate in order to reduce link error rates [33].

D. NEXUS 3

In 2016, Naval Postgraduate School collaborated with SA Photonics, Inc., to explore their NEXUS 3 FSO system aboard Camp Roberts during JIFX 16-3. The purpose of the experiment was to analyze the feasibility of using the commercial NEXUS 3 system (Figure 27) to support tactical operations, specifically with regard to distance. Similar to the Space Photonics LaserFire system, the NEXUS 3 was originally designed for use in short distance FSO

communications between commercial buildings. However, tactical testing during JIFX proved more successful than with LaserFire. The system was effective at up to 10 kilometers with a throughput of 9.6 Gbps [4]. While the overall results of the testing were limited, the experimentation of the NEXUS 3 demonstrate that certain commercial FSO systems offer promising solutions to tactical FSO requirements.

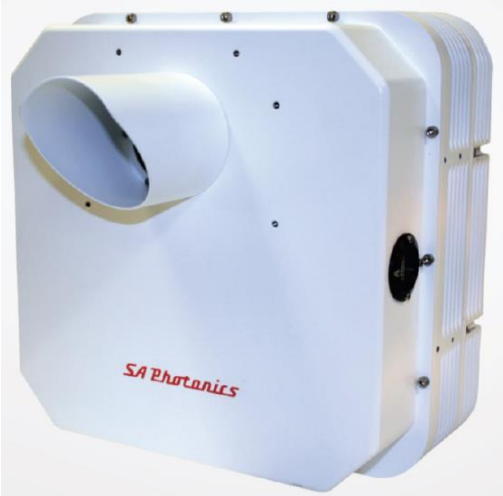

Figure 27. SA Photonics NEXUS 3 Terminal. Source: [4].

E. TACTICAL LINE-OF-SIGHT OPTICAL NETWORK (TALON)

TALON is a FSO transmission system being developed by NRL at the request of Marine Corps Systems Command (Figure 28). It seeks to augment current Marine Corps LOS network communications systems, including the UHF digital radio, MRC-142, by providing an FSO system that can provide a high bandwidth link up to and beyond 35 nautical miles. Testing of the prototype TALON system has been conducted at both Marine Corps Base Camp Pendleton and Naval Air Weapons Station China Lake. The longest link that was accomplished was 50 kilometers at a data rate of 214 Mbps (China Lake). The highest bandwidth link achieved was 880 Mbps at 16 kilometers (Camp Pendleton). It should be noted that this maximum bandwidth was limited by the

KG-175D encryption devices used on the link. With a more advanced encryption device, usable data rates in excess of 1 Gbps are expected [11].

Figure 28. Comparison of MRC-142 Antenna (Left) with TALON Transceiver (Right). Source: [11].

NRL is currently working on developing a production level TALON system. The Marine Corps hopes to field the system to augment the MRC-142 in 2019 [11].

THIS PAGE INTENTIONALLY LEFT BLANK

APPENDIX B. QR ENCODING

The QR Code was developed in 1994 by DENSO ADC Corporation as a replacement for conventional 1-dimensional bar codes. The 2-dimensional code is able to contain denser machine-readable information in a smaller space than similar codes. An example of a QR code is shown in Figure 29. The original QR code, Version 1, was 21-by-21 pixels and able to hold up to 152 bits of data, as discussed below [6]. Since the inception of this original QR code, 40 total QR versions have been developed, the largest of which having dimensions of 177 by 177 pixels. It is a recognized standard by the International Organization for Standardization in standard ISO/IEC 18004 [6].

Figure 29. Example 21 by 21 QR Code. Source: [7].

A. STRUCTURE

Much of the value of the QR codes is derived from its uniform format between different versions. While the 40 different versions possess different capacities for data, they all contain certain uniform aspects, as shown in Figure 30.

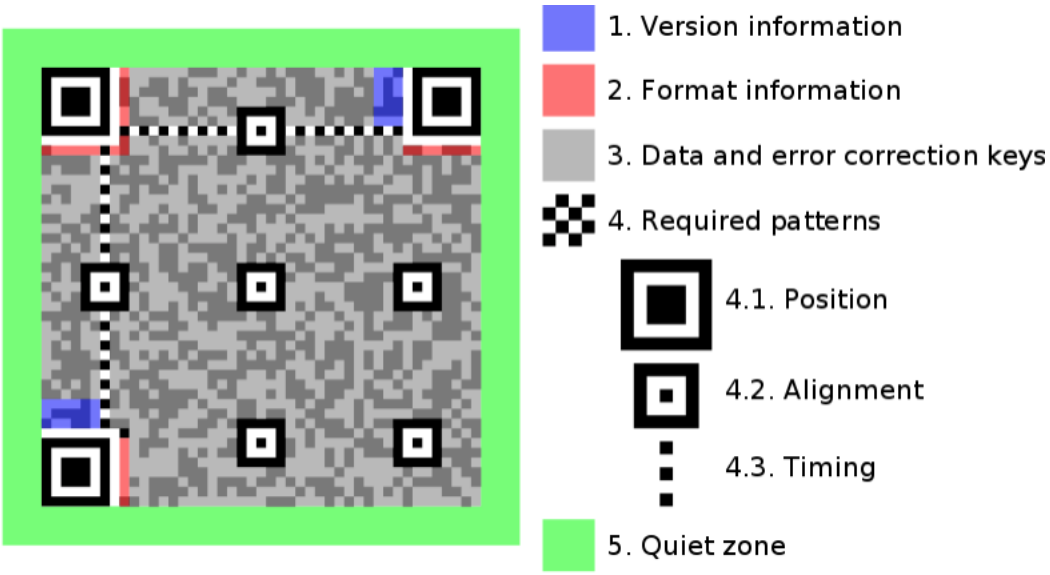

Figure 30. Anatomy of QR Code. Source: [6].

While the majority of a QR image is dedicated to carrying data, there are four standardized types of marking in the image that are used for signaling to the device reading the code: version information, format information, required patterns, and the quiet zone. Because many of these signaling standards require the same amount of pixels no matter what QR version is being used, smaller QR versions dedicate a much higher percentage of the overall image to signaling than larger QR versions do. For example, a Version 1 QR code uses 273 pixels of its 441-pixel image for signaling (61.9%), while a Version 40 QR code only uses 1135 of its 31329 pixels for this purpose (3.6%) [6].

1. Version Information

Shown in blue in Figure 30, the version information identifies what QR code version the image is using, ranging from 1 to 40. In total, 36 pixels of every QR code are dedicated to this information.

2. Format Information

Shown in red in Figure 30, the format information identifies the mask of the code and the error correction value, Low, Medium, Quartile or High. Every QR code utilizes 35 pixels for displaying this information.

3. Required Patterns

Every QR code has two required patterns, position and timing, and one optional pattern, alignment.

a. Position

The position patterns are the most distinctive aspect of any QR code; black and white boxes located at the top two corners and bottom left corner of the image. At 64 pixels each, every QR code dedicates 192 pixels to this patterns. The purpose of the pattern is to quickly allow a QR code reader to identify and orient the code in order to scan it.

b. Timing

The timing lines in the QR code are located between the top two position patterns and the left two position patterns. Their purpose is to assist the QR code reader with determining the coordinates of the image by providing spacing synchronization between position patterns [6]. The total pixels used for this pattern vary between versions.

c. Alignment

The alignment pattern is present in QR version 2 and higher. It is used to detect any curvature or distortion to the code, allowing the reader to make corrections as needed. For larger QR versions, multiple alignment patterns may be included, as shown in Figure 30.

4. Quiet Zone

A buffer around the edge of every QR code, known as the quiet zone, is recommended for optimal reading. It is recommended that the zone has a width of four pixels relative to the QR code; however, it is possible for QR scanners to read the code with less depending on the conditions. The Quiet Zone effectively “frames” the coded data

B. DATA

Data can be encoded into the QR format in four ways; numeric, alphanumeric, binary, and kanji. Each method of encoding supports different sets of characters and different data capacities.

1. Numeric

Numeric encoding supports the use of the ten numeric digits to encode data. It is the most efficient type of QR encoding and provides the largest capacity for QR codes. It only supports the use of integers and has no provisions for encoding negative or fractional numbers, making it less practical than some other encoding formats [27].

2. Alphanumeric

This type of encoding builds on numeric coding by adding uppercase letters, the horizontal space, and eight punctuation characters to the set of characters that can be encoded. It is less efficient than numeric encoding but often more practical, being able to support entire URLs and other strings [27]. This thesis leverages alphanumeric strings to encode hexadecimal values in QR codes.

3. Binary

Binary is the least efficient method of encoding data in a QR code due to the minimal number of characters supported. It simply uses strings of 1s and 0s to represent data [27].

4. Kanji

Kanji was included as an encoding type due to Denso Wave being a Japanese company. While Kanji encoding actually supports fewer characters than binary encoding per QR code, it is more efficient due to the fact that Kanji characters often represent entire words or phrases [27].

C. ERROR CORRECTION

QR codes have inherent error correction ranging from 7% to 30%. This enables them to be read if the image is distorted or part of the code is torn or obscured. There are four ECC levels; Low, with 7% correction; Medium, with 15% correction; Quartile, with 25% correction; and High, with 30% correction [6].

D. INTEGRATING WITH FSO

The QR code format is appealing for using with MIMO FSO transmitters because of the standard's inherent error correction, scalability, and accessibility. However, there are multiple characteristics of the format that are sub-optimal for MIMO FSL implementation that may able to be improved upon.

1. Required Patterns and Standards May Be Unnecessary for FSO Use

While the alignment, timing, and position patterns are valuable for one-time-use QR codes, these standards may be unnecessary for MIMO FSO use. It can be reasonably assumed that after reading the first QR code in a MIMO optical link that all following FSO codes will be of the same alignment and position, reducing the need for such robust signaling dedicated to this purpose.

Similarly, the inclusion of the QR version in every image is likely redundant because QR MIMO links will likely maintain the same version for the entire duration of the link.

The same cannot be said for the format information. Possible QR MIMO employment includes the continuous variation of ECC levels to adapt the link to

changing atmospheric conditions. Because of this, format information should be included in every QR image.

2. Quiet Space Requirement Inefficient

The need for an optical QR image to have a border of Quiet Space greatly increases the number of diodes required. In the tested QOTR/LED system, QR Version 3 images were used, measuring 29 by 29 pixels, but to display them an array of 31 by 31 diodes was required to accommodate buffer space. In a printed QR code this dimension increase is not significant, but when projecting optically this requires an additional 120 diodes for QR Version 3 that are not used for payload transmission. An optimal QR-style format for MIMO FSO would require no Quiet Space diodes to be properly received.

APPENDIX C. CONCEPTS OF EMPLOYMENT

This section offers descriptions of various link architectures that MIMO FSO systems may support.

A. POINT-TO-POINT

Point-to-point, shown in Figure 31, is the typical link topology used for wideband area network (WAN) links. One of the primary envisioned usages for FSO links is to provide WAN connectivity, making point-to-point an obvious choice for employment. This topology offers the advantage of being symmetric and easy to use in full duplex mode. Both ends of the link have identical transmitters and receivers. However, dependent on the nature of optical waves, any FSO point-to-point link is going to be limited by critical LOS.

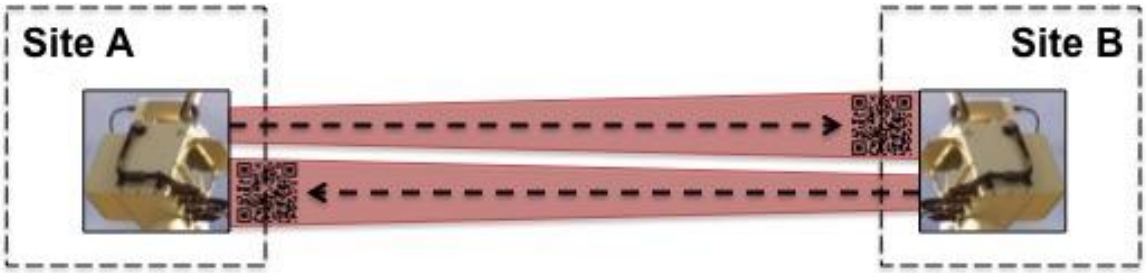

Figure 31. FSO Point-to-Point Link Topology.

Compared to point-to-point RF links, FSO offers the advantage of not needing multiple frequencies to accomplish a full duplex link. Yet, unlike RF link topologies, FSO is not able to achieve a point-to-multipoint configuration using only one transceiver as a hub because of the tight beam divergence of optical waves.

B. REPEATER

A common way to overcome the limitations of a LOS link is to use repeater sites, chaining multiple LOS links together, as shown in Figure 32. With

the high bandwidth capabilities of FSO, this is a valuable method for achieving long-range WAN connectivity. As with RF repeaters, in a tactical environment this requires more manpower to secure intermediate locations to serve as repeater sites, however the power and equipment requirements will be lower because of the footprint of FSO systems. Additionally, it would provide the site with a lower emissions signature.

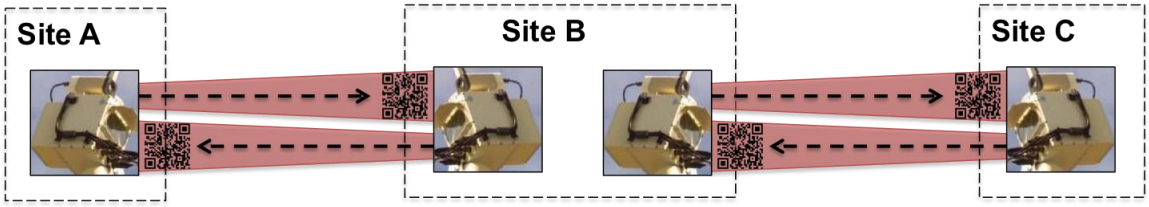

Figure 32. FSO Repeater Link Topology.

C. INDIRECT LINE-OF-SIGHT

Indirect Line-of-Sight (ILOS) is a new concept being introduced in this thesis for application with MIMO FSO systems. ILOS seeks to overcome physical obstacles that block LOS transmission by projecting the MIMO image on an adjacent object that both the sender and receiver can see. The concept is shown in Figure 33. The built-in error correction used in each MIMO QR code can help overcome any optical interference caused by the indirect projection. Examples of ILOS projection surfaces could include building walls, aero-vehicles, still water surfaces, and ships. Depending on atmospherics, the MIMO patterns could theoretically be projected on low-lying clouds. Projections could also be done through transparent screens or glass panels in order to create angles in the link.

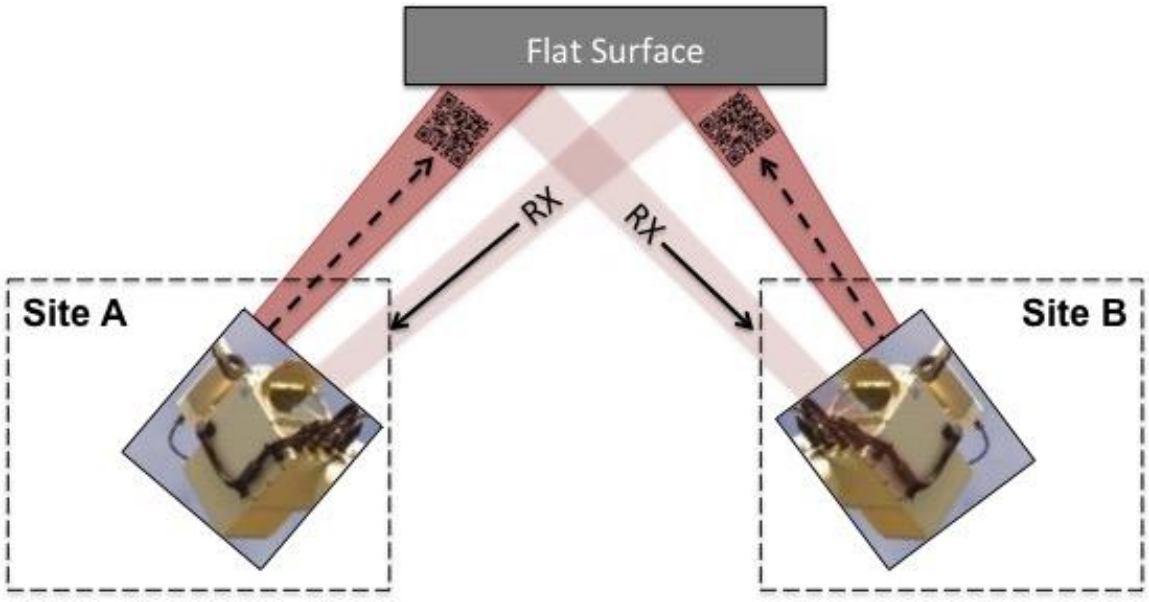

Figure 33. Indirect-Line-of-Sight FSO Link Topology.

While offering the ability to overcome environmental obstacles, ILOS has the limitation of being simplex in nature. It may be necessary for the projection surface to be located closer to the receiver than the transmitter because of the optical receiver's capabilities. For a full duplex employment to work it would likely require a different projection surface to be used for each direction of the link. Despite this, the ILOS simplex configuration could still be valuable for communicating things like UAV feeds to distant units that only need to be receive-only.

D. MIMO BROADCAST

Employing MIMO FSO in a broadcast configuration and leveraging the ILOS concept provides a simplex point-to-multipoint scenario where the transmitter displays the MIMO image on a surface that multiple receivers can read, as shown in Figure 34. This could be valuable in a tactical situation where various subordinate units need to pull down uniform situational updates.

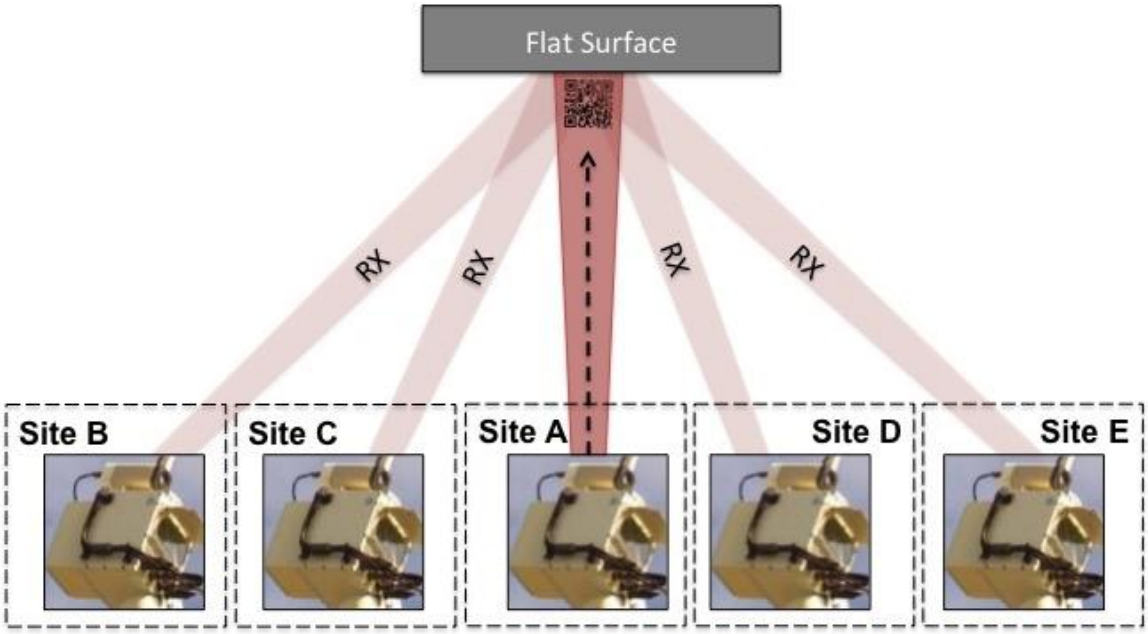

Figure 34. FSO MIMO Broadcast Link Topology.

The broadcast concept has multiple significant implications about networking. First, due to the architecture working in a simplex mode, the scenario would be restricted to UDP network traffic. Modifications would also have to be made on the receiver nodes as there would be no way to conduct signaling back to the transmitter nodes. Additionally, validation of who is allowed to read the broadcast data would be important to manage. While this could be done with standard military cryptography devices, these permissions could also be ingrained in the link layer protocol, however, this would likely require a new type of addressing scheme.

APPENDIX D: QOTR / LED EXPERIMENTATION RESULTS

This appendix provides the full results of the testing conducted on the QOTR/LED system. Testing was conducted on the system by varying the ECC level of the QOTR link between Low, Medium, Quartile, and High. Ten trials were conducted for each ECC level. The distance between the transmitter and the receiver remained constant at 1 foot and network traffic was provided from a randomly generated PCAP on the NPS network. The results are broken into two tables. Table 6 shows the results of the ECC level Low and Medium trials and Table 7 shows the results of the ECC level Quartile and High trials.

The data in the tables is broken into four sections. “Packets” displays metrics collected on the amount of overall network packets sent and received during the trial. “Frames” displays metrics collected on the QOTR frames sent and received and also includes calculated frame transmission rates. “Bytes” includes both metrics collected on the transmission of bytes during the trials as well as additional values calculated to assist with further characterization of link performance. Lastly, “Metrics” includes the calculated values of FER, PER, BER, and the frame usage that was calculated from other values with the results.

Table 6 QOTR/LED Experimentation Results (Part 1).

			Packets		Frames					Bytes						Metrics				
	Trial	Time (sec)	Sent	Received	Sent	Received	Used	Tx Speed (FPS)	Rx Speed (FPS)	Tx Capacity (Bytes)	Rx Capacity (Bytes)	Sent (Bytes)	Received (Bytes)	Tx Speed (Bps)	Rx Speed (Bps)	BER	Send Usage	PER	FER	Avg Packet Size (Bytes)
ECC M	*AVG*	309.1	44.8	44.5	1146	1145	1129	3.71	3.71	31501.3	31493.0	30801.6	30414.5	99.65	98.41	1.26%	97.78%	0.74%	0.03%	701.67
	1	301	38	38	1152	1152	1152	3.83	3.83	31680.0	31680.0	30912	30912	102.70	102.70	0.00%	97.58%	0.00%	0.00%	813.47
	2	305	51	50	1111	1110	1059	3.64	3.64	30552.5	30525.0	29791	28377	97.68	93.04	4.75%	97.51%	1.96%	0.09%	584.14
	3	324	52	52	1207	1207	1207	3.73	3.73	33192.5	33192.5	32430	32430	100.09	100.09	0.00%	97.70%	0.00%	0.00%	623.65
	4	297	40	39	1092	1091	1042	3.68	3.67	30030.0	30002.5	29465	28095	99.21	94.60	4.65%	98.12%	2.50%	0.09%	736.63
	5	295	48	48	1099	1099	1099	3.73	3.73	30222.5	30222.5	29453	29453	99.84	99.84	0.00%	97.45%	0.00%	0.00%	613.60
	6	341	34	33	1267	1266	1203	3.72	3.71	34842.5	34815.0	34099	33012	100.00	96.81	3.19%	97.87%	2.94%	0.08%	1002.91
	7	309	50	50	1115	1115	1115	3.61	3.61	30662.5	30662.5	29969	29969	96.99	96.99	0.00%	97.74%	0.00%	0.00%	599.38
	8	309	44	44	1142	1142	1142	3.70	3.70	31405.0	31405.0	30736	30736	99.47	99.47	0.00%	97.87%	0.00%	0.00%	698.55
	9	307	45	45	1134	1134	1134	3.69	3.69	31185.0	31185.0	30538	30538	99.47	99.47	0.00%	97.93%	0.00%	0.00%	678.62
	10	303	46	46	1136	1136	1136	3.75	3.75	31240.0	31240.0	30623	30623	101.07	101.07	0.00%	98.02%	0.00%	0.00%	665.72
ECC L	*AVG*	308.3	57.1	54.5	1149	1146	1035	3.73	3.72	40793.1	40690.1	39897.6	35905.9	129.40	116.65	9.84%	97.81%	4.60%	0.25%	724.29
	1	313	67	62	1169	1164	1054	3.73	3.72	41499.5	41322.0	40213	36499	128.48	116.61	9.24%	96.90%	7.46%	0.43%	600.19
	2	305	40	40	1123	1123	1123	3.68	3.68	39866.5	39866.5	39187	39187	128.48	128.48	0.00%	98.30%	0.00%	0.00%	979.68
	3	305	48	46	1131	1129	981	3.71	3.70	40150.5	40079.5	39381	34098	129.12	111.80	13.42%	98.08%	4.17%	0.18%	820.44
	4	336	63	59	1254	1250	945	3.73	3.72	44517.0	44375.0	43575	32683	129.69	97.27	25.00%	97.88%	6.35%	0.32%	691.67
	5	306	67	65	1151	1149	1100	3.76	3.75	40860.5	40789.5	39824	38068	130.14	124.41	4.41%	97.46%	2.99%	0.17%	594.39
	6	315	42	39	1182	1177	1061	3.75	3.74	41961.0	41783.5	41338	37096	131.23	117.77	10.26%	98.52%	7.14%	0.42%	984.24
	7	300	54	48	1119	1113	881	3.73	3.71	39724.5	39511.5	38863	30511	129.54	101.70	21.49%	97.83%	11.11%	0.54%	719.69
	8	300	60	59	1095	1094	1056	3.65	3.65	38872.5	38837.0	38065	36695	126.88	122.32	3.60%	97.92%	1.67%	0.09%	634.42
	9	301	59	56	1132	1128	1009	3.76	3.75	40186.0	40044.0	39157	34849	130.09	115.78	11.00%	97.44%	5.08%	0.35%	663.68
	10	302	71	71	1135	1135	1135	3.76	3.76	40292.5	40292.5	39373	39373	130.37	130.37	0.00%	97.72%	0.00%	0.00%	554.55

Table 7 QOTR/LED Experimentation Results (Part 2).

			Packets		Frames					Bytes						Metrics				
	Trial	Time (sec)	Sent	Received	Sent	Received	Used	Tx Speed (FPS)	Rx Speed (FPS)	Tx Capacity (Bytes)	Rx Capacity (Bytes)	Sent (Bytes)	Received (Bytes)	Tx Speed (Bps)	Rx Speed (Bps)	BER	Send Usage	PER	FER	Avg Packet Size (Bytes)
ECC H	*AVG*	316.5	23.5	23.5	1130	1130	1130	3.57	3.57	16377.8	16377.8	16153.3	16153.3	51.06	51.06	0.00%	98.64%	0.00%	0.00%	708.53
	10	321	21	21	1140	1140	1140	3.55	3.55	16530.0	16530.0	16326	16326	50.86	50.86	0.00%	98.77%	0.00%	0.00%	777.43
	9	305	19	19	1108	1108	1108	3.63	3.63	16066.0	16066.0	15778	15778	51.73	51.73	0.00%	98.21%	0.00%	0.00%	830.42
	8	320	23	23	1127	1127	1127	3.52	3.52	16341.5	16341.5	16111	16111	50.35	50.35	0.00%	98.59%	0.00%	0.00%	700.48
	7	311	28	28	1097	1097	1097	3.53	3.53	15906.5	15906.5	15763	15763	50.68	50.68	0.00%	99.10%	0.00%	0.00%	562.96
	6	341	20	20	1192	1192	1192	3.50	3.50	17284.0	17284.0	16983	16983	49.80	49.80	0.00%	98.26%	0.00%	0.00%	849.15
	5	326	24	24	1156	1156	1156	3.55	3.55	16762.0	16762.0	16541	16541	50.74	50.74	0.00%	98.68%	0.00%	0.00%	689.21
	4	301	29	29	1137	1137	1137	3.78	3.78	16486.5	16486.5	16251	16251	53.99	53.99	0.00%	98.57%	0.00%	0.00%	560.38
	3	303	17	17	1058	1058	1058	3.49	3.49	15341.0	15341.0	15199	15199	50.16	50.16	0.00%	99.07%	0.00%	0.00%	894.06
	2	315	30	30	1146	1146	1146	3.64	3.64	16617.0	16617.0	16356	16356	51.92	51.92	0.00%	98.43%	0.00%	0.00%	545.20
	1	322	24	24	1134	1134	1134	3.52	3.52	16443.0	16443.0	16225	16225	50.39	50.39	0.00%	98.67%	0.00%	0.00%	676.04
ECC Q	*AVG*	323.4	33.4	33.4	1148	1148	1148	3.55	3.55	23529.9	23529.9	23043.4	23043.4	71.21	71.21	0.00%	97.93%	0.00%	0.00%	706.02
	10	311	34	34	1099	1099	1099	3.53	3.53	22529.5	22529.5	21934	21934	70.53	70.53	0.00%	97.36%	0.00%	0.00%	645.12
	9	342	28	28	1203	1203	1203	3.52	3.52	24661.5	24661.5	24121	24121	70.53	70.53	0.00%	97.81%	0.00%	0.00%	861.46
	8	332	39	39	1195	1195	1195	3.60	3.60	24497.5	24497.5	23961	23961	72.17	72.17	0.00%	97.81%	0.00%	0.00%	614.38
	7	310	31	31	1102	1102	1102	3.55	3.55	22591.0	22591.0	22111	22111	71.33	71.33	0.00%	97.88%	0.00%	0.00%	713.26
	6	306	35	35	1065	1065	1065	3.48	3.48	21832.5	21832.5	21347	21347	69.76	69.76	0.00%	97.78%	0.00%	0.00%	609.91
	5	323	34	34	1130	1130	1130	3.50	3.50	23165.0	23165.0	22688	22688	70.24	70.24	0.00%	97.94%	0.00%	0.00%	667.29
	4	304	29	29	1052	1052	1052	3.46	3.46	21566.0	21566.0	21164	21164	69.62	69.62	0.00%	98.14%	0.00%	0.00%	729.79
	3	319	25	25	1132	1132	1132	3.55	3.55	23206.0	23206.0	22896	22896	71.77	71.77	0.00%	98.66%	0.00%	0.00%	915.84
	2	357	34	34	1292	1292	1292	3.62	3.62	26486.0	26486.0	26049	26049	72.97	72.97	0.00%	98.35%	0.00%	0.00%	766.15
	1	330	45	45	1208	1208	1208	3.66	3.66	24764.0	24764.0	24163	24163	73.22	73.22	0.00%	97.57%	0.00%	0.00%	536.96

THIS PAGE INTENTIONALLY LEFT BLANK

LIST OF REFERENCES

[1] O. Bouchet, *Wireless Optical Telecommunications*, 1st ed. Hoboken, NJ, USA: John Wiley & Sons, Inc, 2012.

[2] S. Kruger and J. C. Charlier, "Long-wavelength VCSELs ready to benefit 40/100-GbE modules," Lightwave, January 12, 2012. [Online]. Available: https://www.lightwaveonline.com/articles/print/volume-28/issue-6/technology/long-wavelength-vcsel-technology-improves.html

[3] A. K. Majumdar, *Advanced Free Space Optics (FSO): A Systems Approach*. New York, NY, USA: Springer, 2015.

[4] J. W. Lai, "Free space optical communcation for tactical operations," M.S. thesis, Computer Science Dept., NPS, Monterey, CA, USA, 2016. [Online]. Available: https://calhoun.nps.edu/handle/10945/50573

[5] W. S. Rabinovich, R. Mahon, M. S. Ferraro, P. G. Goetz, and J. Murphy, "Diversity effects in modulating retro-reflector links," in *SPIE Defense + Security,* 2014. [Online]. Available: https://www.spiedigitallibrary.org/conference-proceedings-of-spie/9080/90801B/Diversity-effects-in-modulating-retro-reflector-links

[6] *Information technology—Automatic identification and data capture techniques—QR Code bar code symbology specification*, ISO/IEC 18004:2015, February, 2015. [Online] Available: https://www.iso.org/standard/62021.html

[7] "QR code essentials," DENSO Wave Incorporated. Accessed March 20, 2018. [Online]. Available: http://www.nacs.org/LinkClick.aspx?fileticket=D1FpVAvvJuo%3D

[8] M. S. Ferraro, W. Freeman, P. G. Goetz, R. Mahon, C. I. Moore, J. L. Murphy, J. Overfield, W. S. Rabinovich, W. R. Smith, M. R. Suite, L. M. Thomas, B. B. Xu, and H. R. Burris, "Tactical network demonstration with free space lasercomm," in *SPIE LASE*, 2011. [Online]. Available: https://www.spiedigitallibrary.org/conference-proceedings-of-spie/7923/792305/Tactical-network-demonstration-with-free-space-lasercomm/10.1117/12.879476.full

[9] W. S. Rabinovich, C. I. Moore, R. Mahon, P. G. Goetz, H. R. Burris, M. S. Ferraro, J. L. Murphy, G.C. Gilbreath M. Vilcheck, and M. R. Suite, " Free-space optical communications research and demonstrations at the U.S. Naval Research Laboratory," *Applied Optics*, vol. 54, no. 31, September 2015. [Online]. Available: https://www.osapublishing.org/ao/ fulltext.cfm? uri=ao-54-31-F189&id=326774

[10] P. G. Goetz, W. S. Rabinovich, R. Mahon, J. L. Murphy, M. S. Ferraro, M. R. Suite, W. R. Smith, B. B. Xu, H. R. Burris, C. I. Moore, W. W. Schultz, " Modulating retro-reflector lasercom systems at the Naval Research Laboratory," in *MILCOM*, 2010. [Online]. Available: https://ieeexplore. ieee.org /document/5680205/

[11] L. Thomas, presentation slides, April 10, 2017.

[12] A. G. Alkholidi and K. S. Altowij, “Free space optical communications—Theory and practices,” in *Contemporary Issues in Wireless Communications*, M. Khatib, Ed. London, UK: InTech, 2014, pp. 159-212.

[13] “APL demonstrates high-bandwidth communications capability at sea,” Johns Hopkins Applied Physics Laboratory, August 24, 2017. [Online]. Available at: http://www.jhuapl.edu/newscenter/pressreleases/2017/ 170824b.asp

[14] C. Chang, C. Li, and H. Lu, "A 100-Gb/s multiple-input multiple-output visible laser light communication system," *IEEE Transactions on Vehicular Technology*, vol. 61, no. 3, March 2012. [Online]. Available: https://ieeexplore.ieee.org/document/6937061/

[15] S. G. Wilson, M. Brandt-Pearce, Q. Cao, and J. H. Leveque, "Free-space optical MIMO transmission with Q-ary PPM," *IEEE Transactions on Communcations*, vol. 53, no. 8, August 2005. [Online]. Available: https://ieeexplore.ieee.org/document/1495861/

[16] H. Ivanov, E. Leitgeb, T. Plank, P. Bekhrad, and T. Mitsev, " Link budget optimization of free space optical systems in relation to the beam diverging angle," in *13th International Conference on ConTEL*, 2015. [Online]. Available: https://ieeexplore.ieee.org/document/7231195/

[17] M. K. Singh, V. Kapoor, V. Setia, and R. Sihag, "Power budget performances of free space optical link using direct line of sight propogation," in *International Journal of Computer Applications*, 2011. [Online]. Available: https://www.ijcaonline.org/specialissues/iceice/number3/4266-iceice020

[18] iX Cameras, *i-SPEED 726: The ultimate high-resolution, high-speed camera*, DS-726-01.26.18, 2018. [Online]. Available: https://www.ix-cameras.com/downloads/726-Datasheet.pdf

[19] Vision Research, *Phantom v2640*, 2018. [Online]. Available: http://www.phantomhighspeed.com/Portals/0/Docs/DS/DS_WEB-v2640.pdf?ver=2018-01-31-112829-730

[20] A-Tech Instruments Ltd., *Memrecam HX-3 high speed camera system*, 2018. [Online]. Available: http://www.a-tech.ca/Product/Series/1641/HX-3_ Ultra_ High_ Speed_Camera/?tab=6

[21] K. W. Ross and J. F. Kurose, *Computer Networking: A Top Down Approach*, 6th ed., Upper Saddle River, NJ, USA: Pearson Education, 2013.

[22] *IEEE Standard for Ethernet*.: Standard 802.3, 2015, [Online]. Available: http://ieeexplore.ieee.org/stamp/stamp.jsp?tp=&arnumber=7428776

[23] *IEEE Standard for Information technology--Telecommunications and information exchange between systems local and metropolitan area networks*.: Standard 802.11, 2016, [Online]. Available: http://ieeexplore .ieee.org/ stamp /stamp.jsp?tp=&arnumber=7786995

[24] RaspberryPi, *Raspberry Pi 3 Model B*., 2017. [Online]. Available: https://cdn.sparkfun.com/datasheets/Dev/RaspberryPi/2020826.pdf

[25] P. Burgess, “16x32 and 32x32 RGB LED Matrix,” Adafruit Learning Systems, Accessed March 10, 2018. [Online]. Available: htt ps://cdn-learn.adafruit.com/downloads/pdf/32x16-32x32-rgb-led-matrix.pdf

[26] L. Ada, “Adafruit RGB Matrix + Real Time Clock HAT for Raspberry Pi,” Adafruit Learning Systems, Accessed March 10, 2018. [Online]. Available: https://cdn-learn.adafruit.com/downloads/pdf/adafruit-rgb-matrix-plus-real-time-clock-hat-for-raspberry-pi.pdf

[27] M. Nooner, “PyQRCode’s documentation,” Python Hosted, Accessed March 12, 2018. [Online]. Available: http://pythonhosted.org/PyQRCode/index.html

[28] “zbar-py 1.0.4,” The Python Package Index, Accessed March 12, 2018. [Online]. Available: https://pypi.python.org/pypi/zbar-py/1.0.4

[29] “opencv-python 3.4.0.12,” The Python Package Index, Accessed March 12, 2018. [Online]. Available: https://pypi.python.org/pypi/opencv-python /3.4.0.12

[31] “Welcome to Scapy’s documentation,” Read the Docs, Accessed March 12, 2018. [Online]. Available: http://scapy.readthedocs.io/en/latest/

[31] Quarton Inc., *Economical Laser VLM-635/650-03 Series*, 2014. [Online]. Available: https://www.quarton.com/download_list/1/11/30/28/

[32] L. B. Stotts, N. Plasson, T. W. Martin, D. W. Young, and J. Juarez, "Progress towards reliable free-space optical networks," in *MILCOM,* 2011. [Online]. Available: https://ieeexplore.ieee.org/abstract/document/6127559/

[33] C. Casey, "Free space optical communication in the military environment," M.S. thesis, Computer Science Dept., NPS, Monterey, CA, USA, 2014. [Online]. Available: https://calhoun.nps.edu/handle/10945/43886

INITIAL DISTRIBUTION LIST

1. Defense Technical Information Center
   Ft. Belvoir, Virginia

2. Dudley Knox Library
   Naval Postgraduate School
   Monterey, California